Journal of Medicinal Chemistry

ARTICLE

pubs.acs.org/jmc

# *N*-Benzoylated Phenoxazines and Phenothiazines: Synthesis, Antiproliferative Activity, and Inhibition of Tubulin Polymerization

Helge Prinz,*[,†] Behfar Chamasmani,[†] Kirsten Vogel,[†] Konrad J. Böhm,[‡] Babette Aicher,[§] Matthias Gerlach,[§] Eckhard G. Günther,[§] Peter Amon,[∥] Igor Ivanov,[∥] and Klaus Müller[†]

[†]Institute of Pharmaceutical and Medicinal Chemistry, Westphalian Wilhelms-University, Hittorfstrasse 58-62, D-48149 Münster, Germany

[‡]Leibniz Institute for Age Research—Fritz Lipmann Institute (FLI), Beutenbergstrasse 11, D-07745 Jena, Germany

[§]Aeterna Zentaris GmbH, Weismüllerstrasse 50, D-60314 Frankfurt, Germany

[∥]Oncolead GmbH & Co. KG, Fraunhoferstrasse 20, D-82152 Planegg, Germany

Supporting Information

**ABSTRACT:** A total of 53 *N*-benzoylated phenoxazines and phenothiazines, including their *S*-oxidized analogues, were synthesized and evaluated for antiproliferative activity, interaction with tubulin, and cell cycle effects. Potent inhibitors of multiple cancer cell lines emerged with the 10-(4-methoxybenzoyl)-10*H*-phenoxazine-3-carbonitrile (**33b**, $IC_{50}$ values in the range of 2−15 nM) and the isovanillic analogue **33c**. Seventeen compounds strongly inhibited tubulin polymerization with activities higher than or comparable to those of the reference compounds such as colchicine. Concentration-dependent flow cytometric studies revealed that inhibition of K562 cell growth was associated with an arrest in the G2/M phases of the cell cycle, indicative of mitotic blockade. Structure−activity relationship studies showed that best potencies were obtained with agents bearing a methoxy group placed *para* at the terminal phenyl ring and a 3-cyano group in the phenoxazine. A series of analogues highlight not only the phenoxazine but also the phenothiazine structural scaffold as valuable pharmacophores for potent tubulin polymerization inhibitors, worthy of further investigation.

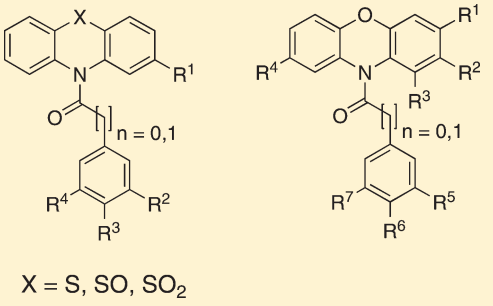


## INTRODUCTION

Microtubules play a key role in organizing the spatial distribution of organelles throughout interphase and of chromsomes during cell division. The mitotic spindle, constituted of microtubules generated by noncovalent polymerization of $\alpha\beta$-tubulin heterodimers, has become an attractive and successful target to treat many types of malignancies.[1,2] Drugs acting on microtubules are of wide structural heterogeneity. Many of these agents work by inhibiting the polymerization of tubulin into microtubules,[3−6] thereby arresting cells in the G2/M phase of the cell cycle, inhibiting cell division and leading to cell death.

One of the best characterized, highly effective inhibitors of tubulin polymerization is colchicine,[7] which is a toxic natural product obtained from *Colchicum autumnale* (**2**). However, obviously due to its narrow therapeutic window, colchicine has not found broad application in anticancer therapy.

So far, the most successful drugs in the clinic have been the *Catharanthus* bis-indole alkaloids vinblastine (**1**, Chart 1) and vincristine.[8] In addition, drugs stimulating tubulin polymerization and stabilizing microtubules such as the taxanes[9] paclitaxel and docetaxel were suitable for the treatment of several cancers, such as ovarian cancer,[10] nonsmall cell lung cancer,[11] and Kaposís sarcoma.[12] Many other natural products, such as combretastatin A-4[13] (**3**) or the epothilones[14] as well as some synthetic molecules including sulfonamide E-7010[15] (**4**), 4-anilinoquinazoline[16] (**5**), anthracenone-derived[17] **6**, 2-methoxyestradiol[18] (**7**), or propenenitrile CC-5079[19] (**8**) (Chart 1) are known to exert their cytotoxic activities through binding to tubulin. The promising usage of microtubule-binding drugs for anticancer therapy stimulated intense efforts aimed at the development of further microtubule-targeting drugs. Therefore, great efforts have recently been made to develop novel small-molecular tubulin binders derived not only from natural sources but also by screening compound libraries in combination with traditional medicinal chemistry.[3,5,20]

We have earlier described a series of anthracenone-derived tubulin polymerization inhibitors with potent in vitro antitumor activity.[17,21−25] Continuing our search strategy for novel, potent tubulin-targeting compounds, we extended our studies to tricyclic heterocycles, which are important scaffolds in medicinal chemistry and a part of numerous important therapeutic agents.[26] Phenothiazine (**9**, Chart 2) and its derivatives have shown diverse biological activities including psychotropic, anticancer,[27] antihelminthic, and other pharmacological properties.[28] 10-Substituted phenothiazines are well-known tranquilizers and

**Received:** April 12, 2011
**Published:** May 12, 2011

ACS Publications © 2011 American Chemical Society

**Chart 1. Examples of Tubulin Interacting Agents**

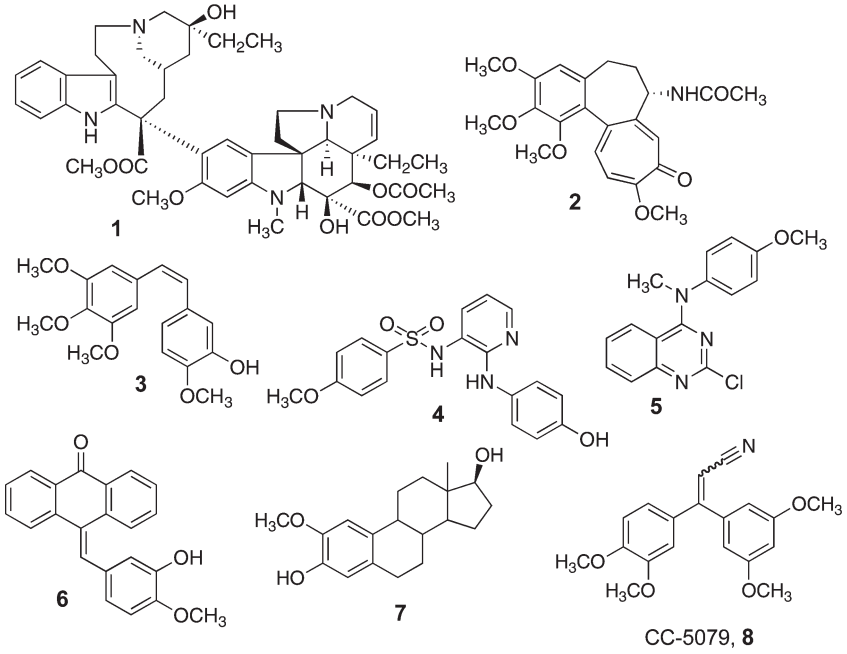


**Chart 2. Phenothiazine (9), Phenoxazine (10), and Related Structures 11, 12, and 13**

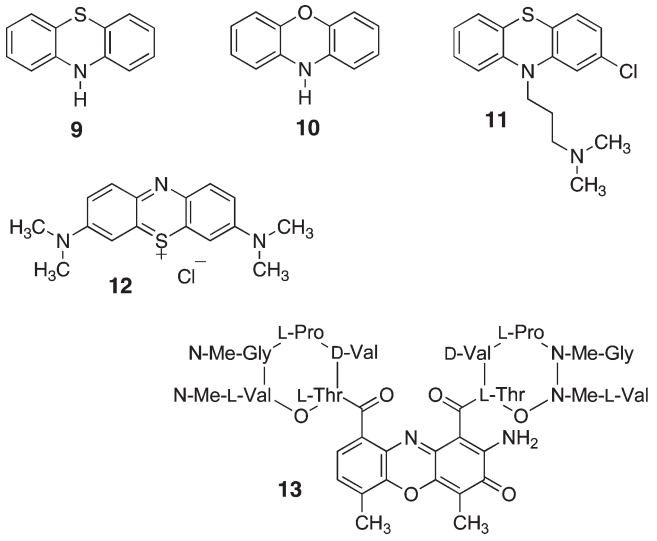


antipsychotic drugs. Chloropromazine (**11**), prepared in 1950, is the prototypical phenothiazine antipsychotic drug and perhaps the best known of the phenothiazine drugs. Phenothiazine dye methylene blue (**12**) is employed as a fast-acting antidote for the treatment of methemoglobinemia.[29] It is also a photosensitizer in the photodynamic therapy of resistant plaque psoriasis.[30] Phenothiazine derivatives have further been demonstrated to induce apoptosis in cultured leukemic cells[31] and to cause mitotic arrest by the inhibition of Eg5 ATPase.[32] Moreover, aryl amide derivatives of phenothiazine are able to inhibit butyrylcholinesterase.[33]

Antitumor activity among phenoxazine (**10**) and its derivatives was not generally known before the discovery of the *Streptomyces*-derived antineoplastic actinomycin polypeptide antibiotics. Actinomycin D (**13**), bearing a phenoxazine chromophore, represents one of the older chemotherapy drugs and is primarily used as an investigative tool in cell biology to inhibit transcription.[34] Meanwhile, the anticancer activities of several phenoxazinones on human leukemia cell lines have also been investigated.[35−37] In addition, *N*-substituted phenoxazines have recently been identified as modulators of MDR[38,39] and as potent specific inhibitors of Akt signaling.[40]

This article reports the synthesis and biological evaluation of *N*-benzoylated phenoxazines and phenothiazines. Some of them demonstrated the ability to strongly inhibit the growth of various tumor cell lines, to act in a cell-cycle-dependent manner, and to be remarkably potent inhibitors of tubulin polymerization. The antitubulin activity of the most active compounds was comparable or superior to those of the reference compounds, such as nocodazole, podophyllotoxin, and colchicine.

## CHEMISTRY

Phenothiazines **9**, **14**, **15**, and **17** (Scheme 1) were available from commercial sources. 2-Methoxy-substituted phenothiazine **16** was obtained from diphenylamine according to a literature protocol.[41] Oxidation resulting in ring sulfoxide metabolites is a common biotransformation pathway for all phenothiazines.[42] Numerous examples of phenothiazines in which the sulfur atom is present in higher oxidation states (sulfoxide and sulfone) can be found in the chemical literature. As these metabolites might contribute to the biological effects of the parent compounds, we were also interested in the biological activities related to these phenothiazine derivatives. 10*H*-Phenothiazine-derived sulfoxides **18a**−**18d** and **18f**−**18h** were obtained by *S*-oxidation using *m*CPBA,[43] whereas sulfone derivatives **19a**−**19d** and **19f**−**19i** have been synthesized from the corresponding phenothiazines by oxidation with hydrogen peroxide in glacial acetic acid.[44] The


dx.doi.org/10.1021/jm200436t |*J. Med. Chem.* 2011, 54, 4247–4263

**Scheme 1**[a]

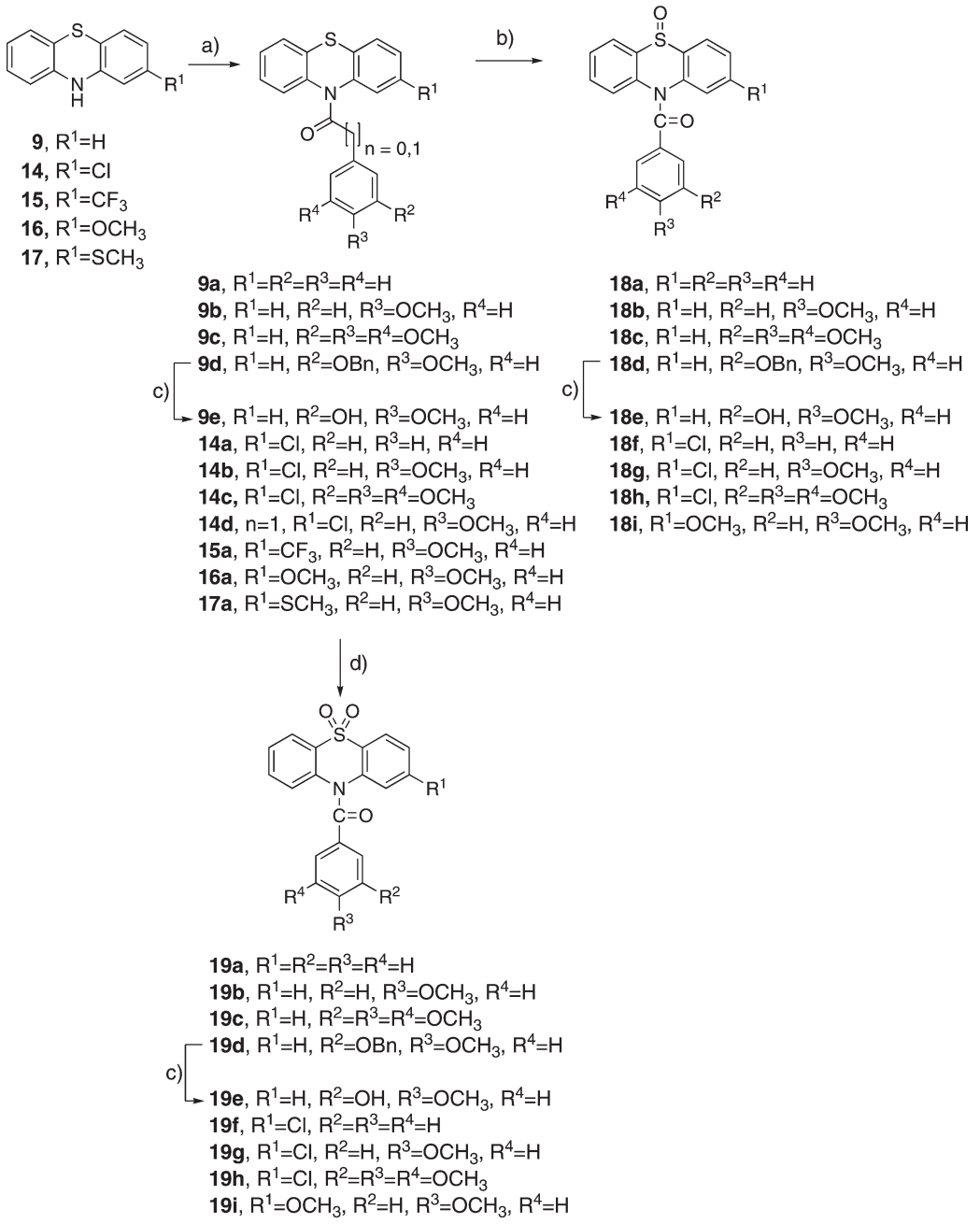


[a] Reagents and conditions: (a) benzoyl chloride, toluene, reflux; (b) *m*CPBA, rt, 12 h; (c) $AlCl_3$, $CH_2Cl_2$, 0 °C; (d) HOAc, $H_2O_2$ 30%, reflux, 2h.

synthesis of carboxamides **9a**−**9d**, **14a**−**14e**, **15a**, **16a**, and **17a** was accomplished by nucleophilic reaction of the respective phenothiazines with appropriately substituted benzoyl chlorides in toluene or benzene, as outlined in Scheme 1. For the synthesis of the isovanillic acid-derived amides **9e**, **18e**, and **19e**, benzyl-protected acid chlorides were reacted with appropriate phenothiazines and their *S*-oxidized analogues in refluxing toluene, followed by the removal of benzyl protection groups using $AlCl_3$ in dichloromethane.[21]

Unsubstituted phenoxazine (**10**) was commercially available. The synthesis of chloro-substituted phenoxazines is depicted in Scheme 2. The starting 2-chloro-10*H*-phenoxazine (**28**) was prepared using a 5-step route according to literature procedures.[38] This classical 2-amino-2′-halodiaryl ether approach was also applied to the synthesis of the 2,8-dichloro-10*H*-phenoxazine (**29**), whereas the 10*H*-phenoxazine carbonitriles **32**, **33**, and **34** were prepared by a cyano-activated fluoro displacement reaction based on a protocol by Eastmond et al.[45] (Scheme 3). Similar to the above-described phenothiazine derivatives, *N*-benzoylation was achieved by reacting the phenoxazines with the respective benzoyl chlorides in refluxing toluene (Scheme 4). Analogues **28e** and **28g** were obtained by debenzylation of **28d** and **28f**, respectively. *N*-Benzoylated **33c** was successfully synthesized from **33** without isolating the


dx.doi.org/10.1021/jm200436t |*J. Med. Chem.* 2011, 54, 4247–4263

**Scheme 2**[a]

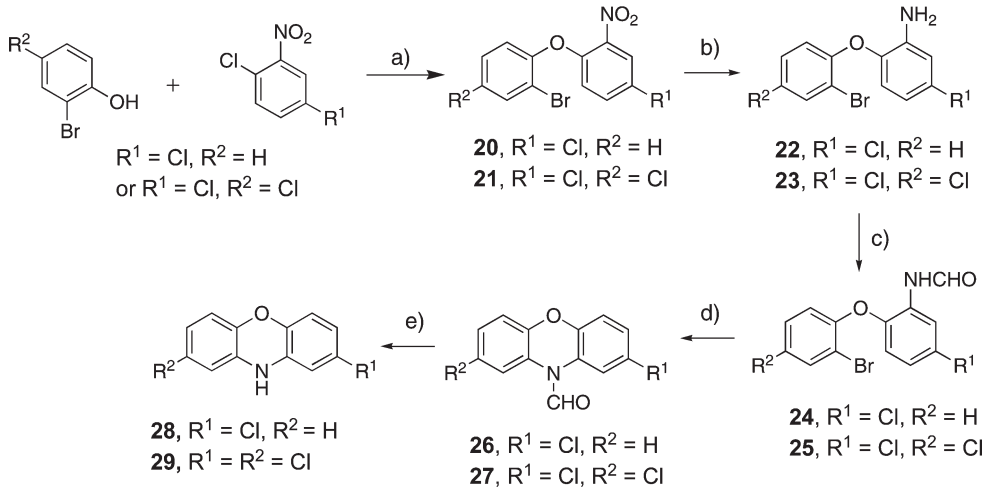


[a] Reagents and conditions: (a) KOH, $H_2O$, 120 °C, 5h; (b) $H_2O$, Fe°, $CH_3COOH$, 90 °C, 3h; (c) HCOOH, 140−160 °C, 4h; (d) $K_2CO_3$, $CuCO_3$, *p*-xylene, reflux; (e) 2N NaOH, toluene, reflux.

**Scheme 3**[a]

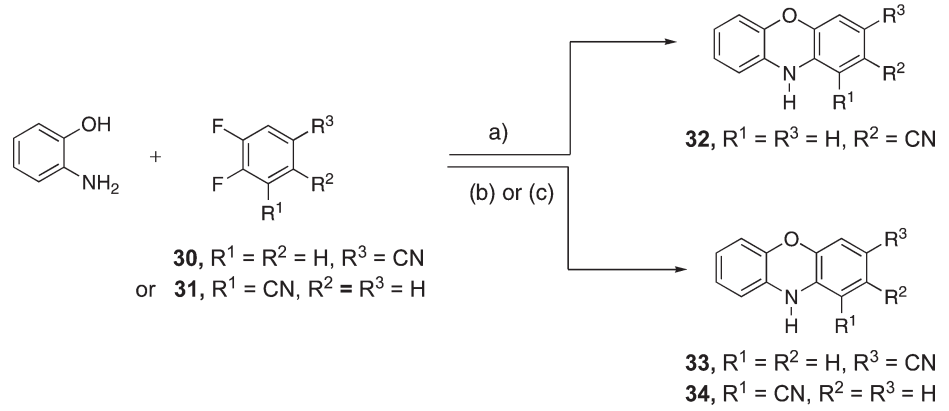


[a] (a) DMF, $K_2CO_3$, toluene, $N_2$, 130 °C; (b) DMSO, $K_2CO_3$, $N_2$, rt; (c) DMF, 170 °C, $N_2$, reflux.

benzyl-protected intermediate (Scheme 4). Synthesis of 2-(2-chloro-phenoxazin-10-yl)-1-(4-methoxyphenyl)-ethanone (**35**) was performed under phase transfer catalysis conditions using 2-bromo-1-(4-methoxyphenyl)ethanone and tetra-*n*-butylammonium bromide (TBAB, Scheme 5).

## BIOLOGICAL RESULTS AND DISCUSSION

**In Vitro Cell Growth Inhibition Assay.** In initial screens with human chronic myelogenous leukemia K562 cells,[46] the compounds were assessed for their ability to inhibit cell proliferation, measured directly by counting the cells with a hemocytometer after 48 h of treatment. Tables 1 and 2 summarize the data for the inhibition of K562 cell growth, compared with the inhibition of tubulin polymerization (see below). Colchicine, nocodazole, podophyllotoxin, vinblastine, and adriamycin served as reference compounds. Our data revealed several interesting aspects including a broad range of potencies. Regarding the phenothiazines and their *S*-oxidized analogues, nine compounds (**9b**, **9e**, **14b**, **16a**, **18b**, **18e**, **19b**, **19e**, and **19g**) showed $IC_{50}$ values in the submicromolar range. The compounds **9a**, **18a**, and **19a**, being unsubstituted in the phenothiazine and in the terminal phenyl ring, were largely devoid of K562 cell growth inhibitory properties ($IC_{50}$ > 30 $\mu$M). Notably, when a methoxy group was introduced at the C-4 position of the terminal phenyl ring, a compound with potency in the submicromolar range (**9b**, $IC_{50}$ 0.33 $\mu$M) was obtained. Regarding the series of 2-chloro-substituted phenothiazines, **14a** and its *S*-oxidized analogues **18f** and **19f** were inactive, whereas *p*-methoxy analogue **14b** displayed submicromolar antiproliferative activity. However, compared with the unsubstituted phenothiazine **9b**, 2-chloro analogue **14b** was considerably less effective (**14b**, $IC_{50}$ 0.84 $\mu$M vs **9b**, $IC_{50}$ 0.33 $\mu$M). Moreover, compound **16a**, being 2-methoxy-substituted in the phenothiazine, presented a cell growth inhibitory activity very similar to that of **14b**. Compared with **9b**, slightly improved potencies were observed for the isovanillic analogues **9e**, **18e**, and **19e**. 10-(3-Hydroxy-4-methoxybenzoyl)-10*H*-phenothiazine (**9e**) was the most active phenothiazine derivative, which inhibited K562 cell growth with an $IC_{50}$ of 0.21 $\mu$M. Interestingly, introduction of a 3,4,5-trimethoxyphenyl group as exemplified in **9c** strongly decreased growth inhibitory properties in comparison with that of 4-methoxyphenyl **9b** and


dx.doi.org/10.1021/jm200436t |*J. Med. Chem.* 2011, 54, 4247–4263

**Scheme 4**[a]

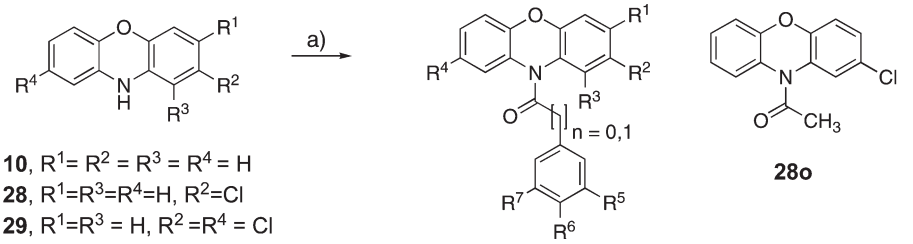


**10**, $R^1 = R^2 = R^3 = R^4 = H$
**28**, $R^1 = R^3 = R^4 = H$, $R^2 = Cl$
**29**, $R^1 = R^3 = H$, $R^2 = R^4 = Cl$
**32**, $R^1 = R^3 = R^4 = H$, $R^2 = CN$
**33**, $R^1 = CN$, $R^2 = R^3 = R^4 = H$
**34**, $R^1 = R^2 = R^4 = H$, $R^3 = CN$

**28o**

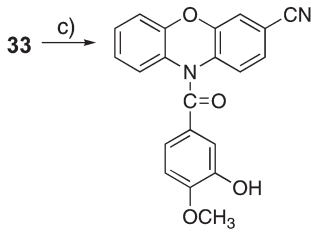


**33c**

**10a**, $R^1 = R^2 = R^3 = R^4 = R^5 = H$, $R^6 = OCH_3$, $R^7 = H$
**10b**, n=1, $R^1 = R^2 = R^3 = R^4 = R^5 = H$, $R^6 = OCH_3$, $R^7 = H$
**28a**, $R^1 = H$, $R^2 = Cl$, $R^3 = R^4 = R^5 = H$, $R^6 = OCH_3$, $R^7 = H$
**28b**, $R^1 = H$, $R^2 = Cl$, $R^3 = R^4 = H$, $R^5 = OCH_3$, $R^6 = R^7 = H$
**28c**, n=1, $R^1 = H$, $R^2 = Cl$, $R^3 = R^4 = R^5 = H$, $R^6 = OCH_3$, $R^7 = H$
**28d**, $R^1 = H$, $R^2 = Cl$, $R^3 = R^4 = H$, $R^5 = OBn$, $R^6 = OCH_3$, $R^7 = H$ (b)
**28e**, $R^1 = H$, $R^2 = Cl$, $R^3 = R^4 = H$, $R^5 = OH$, $R^6 = OCH_3$, $R^7 = H$
**28f**, $R^1 = H$, $R^2 = Cl$, $R^3 = R^4 = H$, $R^5 = OCH_3$, $R^6 = OBn$, $R^7 = OCH_3$ (b)
**28g**, $R^1 = H$, $R^2 = Cl$, $R^3 = R^4 = H$, $R^5 = OCH_3$, $R^6 = OH$, $R^7 = OCH_3$
**28h**, $R^1 = H$, $R^2 = Cl$, $R^3 = R^4 = H$, $R^5/R^6 = OCH_2O$, $R^7 = H$
**28i**, $R^1 = H$, $R^2 = Cl$, $R^3 = R^4 = H$, $R^5 = R^6 = R^7 = OCH_3$
**28j**, $R^1 = H$, $R^2 = Cl$, $R^3 = R^4 = R^5 = H$, $R^6 = CF_3$, $R^7 = H$
**28k**, $R^1 = H$, $R^2 = Cl$, $R^3 = R^4 = R^5 = H$, $R^6 = Cl$, $R^7 = H$
**28l**, $R^1 = H$, $R^2 = Cl$, $R^3 = R^4 = R^5 = H$, $R^6 = Br$, $R^7 = H$
**28m**, $R^1 = H$, $R^2 = Cl$, $R^3 = R^4 = R^5 = H$, $R^6 = N(CH_3)_2$, $R^7 = H$
**28n**, $R^1 = H$, $R^2 = Cl$, $R^3 = R^4 = R^5 = H$, $R^6 = NO_2$, $R^7 = H$
**29a**, $R^1 = H$, $R^2 = Cl$, $R^3 = H$, $R^4 = Cl$, $R^5 = H$, $R^6 = OCH_3$, $R^7 = H$
**32a**, $R^1 = H$, $R^2 = CN$, $R^3 = R^4 = R^5 = H$, $R^6 = OCH_3$, $R^7 = H$
**33a**, $R^1 = CN$, $R^2 = R^3 = R^4 = R^5 = R^6 = R^7 = H$
**33b**, $R^1 = CN$, $R^2 = R^3 = R^4 = R^5 = H$, $R^6 = OCH_3$, $R^7 = H$
**33c**, $R^1 = CN$, $R^2 = R^3 = R^4 = H$, $R^5 = OH$, $R^6 = OCH_3$, $R^7 = H$
**33d**, $R^1 = CN$, $R^2 = R^3 = R^4 = R^5 = H$, $R^6 = Cl$, $R^7 = H$
**34a**, $R^1 = R^2 = H$, $R^3 = CN$, $R^4 = R^5 = H$, $R^6 = OCH_3$, $R^7 = H$

[a] Reagents and conditions: (a) benzoyl chloride, acetyl chloride in the case of **28o**, toluene, reflux; (b) $AlCl_3$, 1,2-DCE, 0 °C; (c) (i) 3-benzyloxy-4-methoxybenzoic acid, $(COCl)_2$, 0 °C; (ii) pyridine, reflux; (iii) $AlCl_3$, $CH_2Cl_2$, 0 °C, 4h.

**Scheme 5**[a]

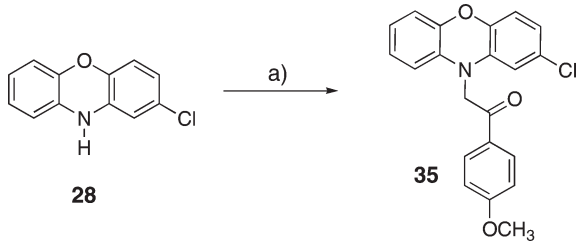


**28**

**35**

[a] Reagents and conditions: (a) TBAB, NaOH 50%/THF, 2-bromo-1-(4-methoxyphenyl)ethanone, rt, 1h.

isovanillic **9e**. Likewise, this finding was reaffirmed by a distinctive loss of activity for 2-chloro-substituted analogue **14c** ($IC_{50}$ 11 $\mu$M) vs **14b**. In general, introduction of 2-substituents into the phenothiazine ring, such as chloro, trifluoromethyl (**15a**, $IC_{50}$ K562 4.60 $\mu$M), methoxy (**16a**), or thiomethyl (**17a**) did not lead to improved activities compared with those of **9b** or **9e**, both being unsubstituted in phenothiazine. Noteworthy, inserting a methylene spacer between the amide group and the terminal phenyl ring did not cause an activity enhancement but even resulted in a nearly 10-fold reduction of antiproliferative potency (**14b**, $IC_{50}$ 0.84 $\mu$M vs **14d**, $IC_{50}$ 8 $\mu$M).

The more or less similar antiproliferative potencies of phenothiazines and their corresponding sulfoxides and sulfones (**9b** vs **18b**, **19b**; **9c** vs **18c**, **19c**; **9e** vs **18e**, **19e**; **14b** vs **18g**, **19g**; and **16a** vs **18i**, **19i**) allow one to conclude that the sulfur oxidation state has little influence on antiproliferative effects. However, as mentioned above, the formation of sulfoxides and sulfones from phenothiazines is a common metabolizing pathway which cannot be excluded under the conditions of the cellular assay, hence explaining the similar results from the antiproliferative assay. Similar to the phenothiazines **9b** and **9e**, the sulfoxides **18b** ($IC_{50}$ 0.42 $\mu$M) and **18e** ($IC_{50}$ 0.30 $\mu$M), respectively, were the most active. As expected, trimethoxyphenyl-substituted **18c** displayed substantially less activity than the isovanillic **18e**, though both were unsubstituted in the phenothiazine ring. Moreover, the 2-chloro-substituted sulfoxide **18g** was nearly 3-fold less active than **18b** and **18e**, again indicating that introduction of a chloro atom into the 2-position of the tricyclic nucleus did not improve


dx.doi.org/10.1021/jm200436t | J. Med. Chem. 2011, 54, 4247–4263

**Table 1. Antiproliferative Activity of Phenothiazine Derivatives 9a−9e, 14a−14d, 15a, 16a, 17a, 18a−18i, and 19a−19i against K562 Cells and Anti-Tubulin Activities**

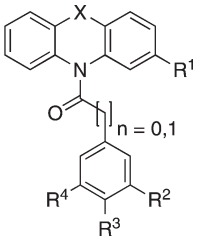


| cmpd | *n* | X | $R^1$ | $R^2$ | $R^3$ | $R^4$ | K562 $IC_{50}$[a] [$\mu$M] | ITP $IC_{50}$[b] [$\mu$M] |
|---|---|---|---|---|---|---|---|---|
| **9** | | | | | | | >100 | ND |
| **14** | | | | | | | >100 | ND |
| **9a** | 0 | S | H | H | H | H | >30 | ND |
| **9b** | 0 | S | H | H | $OCH_3$ | H | 0.33 | 2.23 |
| **9c** | 0 | S | H | $OCH_3$ | $OCH_3$ | $OCH_3$ | 1.86 | 4.96 |
| **9d** | 0 | S | H | OBn | $OCH_3$ | H | >30 | ND |
| **9e** | 0 | S | H | OH | $OCH_3$ | H | 0.21 | 1.40 |
| **14a** | 0 | S | Cl | H | H | H | >30 | ND |
| **14b** | 0 | S | Cl | H | $OCH_3$ | H | 0.84 | 0.87 |
| **14c** | 0 | S | Cl | $OCH_3$ | $OCH_3$ | $OCH_3$ | 11 | >10 |
| **14d** | 1 | S | Cl | H | $OCH_3$ | H | 8 | ND |
| **15a** | 0 | S | $CF_3$ | H | $OCH_3$ | H | 4.60 | >10 |
| **16a** | 0 | S | $OCH_3$ | H | $OCH_3$ | H | 0.97 | 3.23 |
| **17a** | 0 | S | $SCH_3$ | H | $OCH_3$ | H | 3.62 | 1.43 |
| **18a** | 0 | SO | H | H | H | H | >30 | ND |
| **18b** | 0 | SO | H | H | $OCH_3$ | H | 0.42 | 9.39 |
| **18c** | 0 | SO | H | $OCH_3$ | $OCH_3$ | $OCH_3$ | 8.03 | >10 |
| **18d** | 0 | SO | H | OBn | $OCH_3$ | H | ND | ND |
| **18e** | 0 | SO | H | OH | $OCH_3$ | H | 0.30 | 8.40 |
| **18f** | 0 | SO | Cl | H | H | H | >30 | ND |
| **18g** | 0 | SO | Cl | H | $OCH_3$ | H | 1.40 | 2.79 |
| **18h** | 0 | SO | Cl | $OCH_3$ | $OCH_3$ | $OCH_3$ | 35 | >10 |
| **18i** | 0 | SO | $OCH_3$ | H | $OCH_3$ | H | 1.65 | 23.31 |
| **19a** | 0 | $SO_2$ | H | H | H | H | >30 | ND |
| **19b** | 0 | $SO_2$ | H | H | $OCH_3$ | H | 0.28 | 2.53 |
| **19c** | 0 | $SO_2$ | H | $OCH_3$ | $OCH_3$ | $OCH_3$ | 2.60 | 2.46 |
| **19d** | 0 | $SO_2$ | H | OBn | $OCH_3$ | H | ND | ND |
| **19e** | 0 | $SO_2$ | H | OH | $OCH_3$ | H | 0.18 | 3.0 |
| **19f** | 0 | $SO_2$ | Cl | H | H | H | >30 | ND |
| **19g** | 0 | $SO_2$ | Cl | H | $OCH_3$ | H | 0.80 | 1.05 |
| **19h** | 0 | $SO_2$ | Cl | $OCH_3$ | $OCH_3$ | $OCH_3$ | 4.2 | >10 |
| **19i** | 0 | $SO_2$ | $OCH_3$ | H | $OCH_3$ | H | 1.58 | 4.69 |
| colchicine | | | | | | | 0.02 | 1.4 |
| nocodazole | | | | | | | ND | 0.76 |
| podophyllotoxin | | | | | | | ND | 0.35 |
| vinblastine sulfate | | | | | | | 0.001 | 0.13 |
| adriamycin | | | | | | | 0.01 | ND |

[a] $IC_{50}$, concentration of compound required for 50% inhibition of cell growth (K562). Cells were treated with drugs for 48 h. $IC_{50}$ values are the means of at least three independent determinations (SD < 10%). [b] ITP = inhibition of tubulin polymerization; $IC_{50}$ values represent the compound concentration at which the maximum of tubulin assembly level amounts 50% of the level of the control without the compound (determined after 45 min polymerization of tubulin at 37 °C).

the antiproliferative action. Replacement of 2-chloro by methoxy resulted in comparable activities (**18i**, $IC_{50}$ 1.65 $\mu$M vs **18g**, $IC_{50}$ 1.40 $\mu$M). As already observed with the nonoxidized **14c**, the presence of trimethoxy in sulfoxide **18h** induced a dramatic loss of antiproliferative potency ($IC_{50}$ 35 $\mu$M) compared with that of **18g**. In good agreement with the findings from the sulfoxide series, sulfones **19b** and **19e** were the most active analogues.

**Table 2. Antiproliferative Activity of Phenoxazine Derivatives 10a−10b, 28a−28n, 28o, 29a, 32a, 33a−33d, 34a, and 35 against K562 Cells and Anti-Tubulin Activities**

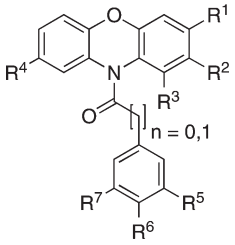


| cmpd | *n* | $R^1$ | $R^2$ | $R^3$ | $R^4$ | $R^5$ | $R^6$ | $R^7$ | K562 $IC_{50}$[a] [$\mu$M] | ITP $IC_{50}$[a] [$\mu$M] |
|---|---|---|---|---|---|---|---|---|---|---|
| **10** | | | | | | | | | >30 | >10 |
| **28** | | | | | | | | | >30 | >10 |
| **33** | | | | | | | | | >10 | >10 |
| **10a** | 0 | H | H | H | H | H | $OCH_3$ | H | 0.033 | 1.10 |
| **10b** | *1* | H | H | H | H | H | $OCH_3$ | H | 4.81 | >10 |
| **28a** | 0 | H | Cl | H | H | H | $OCH_3$ | H | 0.14 | 0.57 |
| **28b** | 0 | H | Cl | H | H | $OCH_3$ | H | H | 1.38 | 0.65 |
| **28c** | 1 | H | Cl | H | H | H | $OCH_3$ | H | 0.55 | 1.10 |
| **28d** | 0 | H | Cl | H | H | OBn | $OCH_3$ | H | ND | ND |
| **28e** | 0 | H | Cl | H | H | OH | $OCH_3$ | H | 0.08 | 0.73 |
| **28f** | 0 | H | Cl | H | H | $OCH_3$ | OBn | $OCH_3$ | ND | ND |
| **28g** | 0 | H | Cl | H | H | $OCH_3$ | OH | $OCH_3$ | 4.63 | 0.68 |
| **28h** | 0 | H | Cl | H | H | $OCH_2O$ | | H | 1.12 | 1.13 |
| **28i** | 0 | H | Cl | H | H | $OCH_3$ | $OCH_3$ | $OCH_3$ | 24 | ND |
| **28j** | 0 | H | Cl | H | H | H | $CF_3$ | H | >75 | ND |
| **28k** | 0 | H | Cl | H | H | H | Cl | H | 20 | 2.42 |
| **28l** | 0 | H | Cl | H | H | H | Br | H | >25 | ND |
| **28m** | 0 | H | Cl | H | H | H | $N(CH_3)_2$ | H | 1.21 | 0.88 |
| **28n** | 0 | H | Cl | H | H | H | $NO_2$ | H | >80 | 5.03 |
| **28o** | | | | | | | | | >30 | ND |
| **29a** | 0 | H | Cl | H | Cl | H | $OCH_3$ | H | 0.49 | 0.70 |
| **32a** | 0 | H | CN | H | H | H | $OCH_3$ | H | 0.16 | 2.70 |
| **33a** | 0 | CN | H | H | H | H | H | H | 0.23 | 1.2 |
| **33b** | 0 | CN | H | H | H | H | $OCH_3$ | H | 0.014 | 0.73 |
| **33c** | 0 | CN | H | H | H | OH | $OCH_3$ | H | 0.011 | 0.52 |
| **33d** | 0 | CN | H | H | H | H | Cl | H | 0.49 | 2.39 |
| **34a** | 0 | H | H | CN | H | H | $OCH_3$ | H | 0.12 | 0.96 |
| **35** | | | | | | | | | >20 | |

[a] For details, see the footnotes in Table 1.

Regarding the phenoxazines, the 10-(4-methoxybenzoyl)-10*H*-phenoxazine (**10a**) showed strong antiproliferative potency with an $IC_{50}$ of 33 nM, thus being 10-fold more active than phenothiazine **9b** ($IC_{50}$ 0.33 $\mu$M). Compound **10a** had no substitution on the phenoxazine ring. Inserting a spacer as exemplified in **10b** caused a dramatic loss of potency. 2-Chloro-[10-(3-hydroxy-4-methoxybenzoyl)]-10*H*-phenoxazin (**28e**), which incorporates the isovanillic partial structures also present in combretastatin A-4 (**3**), also displayed strong antiproliferative activity (**28e**, $IC_{50}$ 0.08 $\mu$M). In addition, compound **28a** was also found to be active ($IC_{50}$ 0.14 $\mu$M). A marked loss in potency was observed for the isomeric **28b**, confirming that a methoxy group placed at the *para*-position of the terminal phenyl is essential, while shifting it to the *meta*-position is detrimental to potency (**28a**, $IC_{50}$ 0.14 $\mu$M vs **28b**, $IC_{50}$ 1.38 $\mu$M). Also, the activity of the dichloro analogue **29a** ($IC_{50}$ 0.49 $\mu$M) was diminished compared to the monochloro **28a**, indicating that introduction of a second chloro atom in phenoxazine (**29a**) did not offer any advantage in terms of potency. Again, insertion of a spacer as seen in 2-chloro-[10-(4-methoxyphenylacetyl)]-10*H*-phenoxazine (**28c**) resulted in about a 4-fold reduction in potency as compared with that of **28a** (**28c**, $IC_{50}$ 0.55 $\mu$M vs. **28a**, $IC_{50}$ 0.14 $\mu$M). Thus, it seems that for the *N*-benzoylated phenothiazines (**14b** vs **14d**; see above) and the phenoxazines (**10a** vs **10b** and **28a** vs **28c**), the spatial disposition of the terminal phenyl ring and the heterocycle is an influential factor in determining antiproliferative activity. The comparison of the $IC_{50}$ values obtained for **28a** with those obtained for *N*-unsubstituted **28** and 10-acetyl-2-chloro-10*H*-phenoxazine (**28o**, Scheme 4) clearly demonstrated that the terminal phenyl ring is essential. The mere


dx.doi.org/10.1021/jm200436t |*J. Med. Chem.* 2011, 54, 4247–4263

**Table 3. Antiproliferative Activity of Phenoxazines 10a, 28a, 28e, 33b and 33c against Different Tumor Cell Lines**

| | $IC_{50}$[a] [$\mu$M] | | | | | | |
|---|---|---|---|---|---|---|---|
| cmpd | NCIH460 | SKOV3 | BT549 | 451LU | SW480 | COLO-205 | DLD-1 |
| **10a** | 0.27 | 0.21 | 0.12 | 0.06 | 0.24 | 0.24 | 0.25 |
| **28a** | 0.68 | 0.35 | 0.33 | 0.09 | 0.53 | 0.43 | 0.54 |
| **28e** | 0.39 | 0.17 | 0.32 | 0.027 | 0.24 | 2.68 | 0.23 |
| **33b** | 0.015 | 0.006 | 0.008 | 0.002 | 0.008 | 0.006 | 0.009 |
| **33c** | 0.04 | 0.024 | 0.016 | 0.006 | 0.029 | ND | 0.016 |
| paclitaxel | 0.004 | 0.006 | 0.006 | 0.006 | 0.011 | 0.005 | 0.05 |
| nocodazole | 0.068 | 0.08 | 0.069 | 0.072 | 0.12 | 0.088 | 0.19 |
| colchicine | 0.027 | 0.029 | 0.023 | 0.017 | 0.030 | 0.021 | 0.089 |

[a] $IC_{50}$ values were determined from Alamar Blue proliferation assays after incubation with the test compound for 48 h. All experiments were performed at least in two replicates ($n = 2$), and $IC_{50}$ data were calculated from dose−response curves by nonlinear regression analysis.

presence of an amide functional group in **28o** of the phenoxazine did not necessarily induce antiproliferative potency ($IC_{50} > 30$ $\mu$M, Table 2). Furthermore, abolishing the amide in the case of **35** (Scheme 5) by inserting a spacer led to a loss of activity as compared with **10a** and **28a**, indicating the importance of the intact amide for potency (**35**, $IC_{50} > 20$ $\mu$M, Table 2). Notably, structure−activity studies showed that antiproliferative potencies of the phenoxazines were ordinarily superior to those of the phenothiazine congeners (e.g., see **10a** vs **9b**; **28a** vs **14b**). A hydroxy group being flanked by methoxy groups in the case of **28g** showed reduced potency ($IC_{50}$ 4.6 $\mu$M). Similar to the aforementioned phenothiazine **9c**, **28i** bearing three methoxy moieties showed a dramatic drop in potency (**28a**, $IC_{50}$ 0.14 $\mu$M vs **28i**, $IC_{50}$ 24 $\mu$M). This is in agreement with similar observations from our previous reports.[17,24,25] The 4,5-methylenedioxy bridge compound **28h** displayed moderate activity comparable to that of the dimethylamino compound **28m**, whereas the halo-substituted analogues **28k** and **28l** were considered to be more or less inactive ($IC_{50}$ values $\geq 20$ $\mu$M). Also, the compounds **28j** and **28n** with an electron-withdrawing trifluoromethyl and nitro group, respectively, revealed a dramatically decreased inhibitory effect on cell growth ($IC_{50} > 70$ $\mu$M) and were assessed to be not active.

Excellent antiproliferative potencies in the phenoxazine series could be attained by introducing a cyano group into the 3-position of the phenoxazine (**33b**, K562 $IC_{50}$ 14 nM; **33c** $IC_{50}$ 11 nM), leading to the most active compounds of all homologues tested. Shifting the cyano group of **33b** to the 1- or 2-position of the phenoxazine, **34a** and **32a**, respectively, resulted in still potent analogues but with decreased potency (**32a**, $IC_{50}$ 0.16 $\mu$M; **34a** $IC_{50}$ 0.12 $\mu$M). However, presently, mechanistic details underlying the impact of the CN group for potency within this series of compounds, such as the importance for molecular recognition or effects on electron densities have not been elucidated yet and are speculative. In this context, several aspects concerning the biological function of the nitrile group reviewed by Fleming et al.[47] might be of interest.

**Effect on Growth of Different Tumour Cell Lines.** Next, to further investigate the antiproliferative potential of tumor cells, the effect of the highly active 3-cyano analogues **33b** and **33c** as well as other potent analogues against a panel of seven cell lines derived from solid tumors was investigated. The antiproliferative activities of the compounds were quantified by the measurement of the cellular metabolic reduction by conversion of the dye Resazurin, yielding a fluorescence signal at 590 nm as indicator of cellular viability.[48] Of the tested compounds, again **33b** displayed outstanding overall antiproliferative activities with $IC_{50}$ values ranging from 2 to 15 nM (Table 3), slightly improved compared to those of colchicine. This outstanding activity of the 3-cyano analogue **33b** is further supported by the colchicine-like activity of the 3-cyano analogue **33c**. Compound **28e** was also effective, though, as expected, its potency was substantially lower than that of **33b** and **33c**.

**Table 4. Most Sensitive and Resistant Cell Lines after Treatment of Solid Tumor Cell Lines with 33c**

| cmpd | **33c** | |
|---|---|---|
| number of tested cell lines | 83 | |
| maximum concentration [$\mu$M] | 10 | |
| mimimum concentration [$\mu$M] | 0.0001 | |
| activity | $GI_{50}$ [$\mu$M] | |
| maximum | 8.4137 | |
| minimum | 0.0018 | |
| mean | 0.0111 | |
| median | 0.0072 | |
| most sensitive cell lines (8 shown) | $GI_{50}$ [$\mu$M] | z-score |
| SKNSH (brain) | 0.0018 | −1.0677 |
| MG63 (bone) | 0.0018 | −1.0601 |
| SKNAS (brain) | 0.0018 | −1.0467 |
| 5637 (bladder) | 0.0019 | −1.0200 |
| RD (muscle) | 0.0020 | −1.0042 |
| SKMEL28 (skin) | 0.0020 | −0.9853 |
| HT1080 (connective tissue) | 0.0026 | −0.8390 |
| A-375 (skin) | 0.0027 | −0.8269 |
| most resistant cell lines (8 shown) | $GI_{50}$ [$\mu$M] | z-score |
| MIAPACA2 (pancreas) | 8.4137 | 3.8507 |
| HT29 (colon) | 5.6032 | 3.6145 |
| COLO205 (colon) | 4.2556 | 3.4546 |
| BXPC3 (pancreas) | 2.2494 | 3.0841 |
| MDAMB436 (breast) | 1.1309 | 2.6845 |
| MT3 (breast) | 0.0951 | 1.2459 |
| IGROV1 (ovary) | 0.0633 | 1.0089 |
| COLO678 (colon) | 0.0623 | 1.0000 |

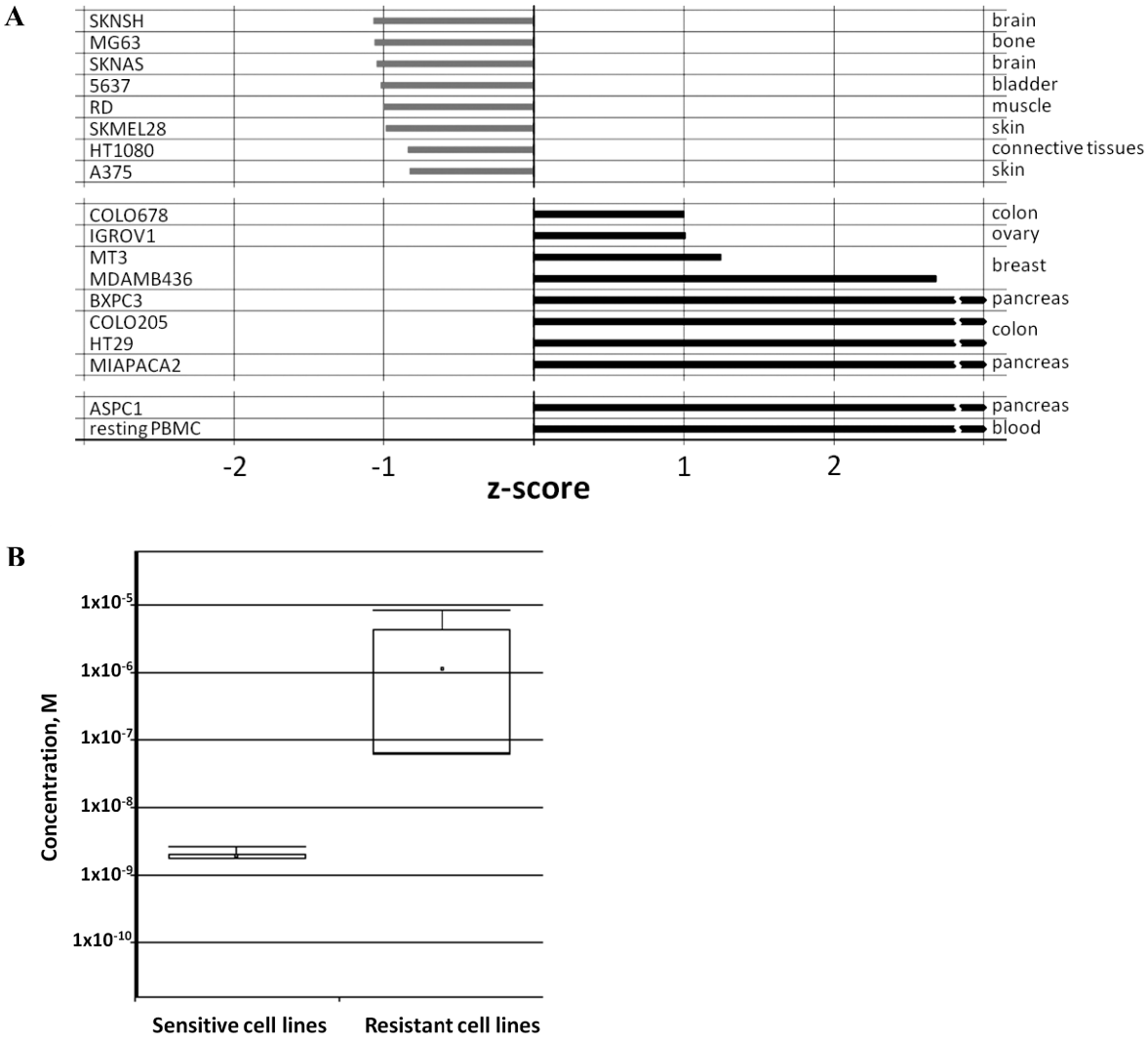


**Figure 1.** (A) Plot of the most sensitive and resistant cell lines (8 are shown each) from the panel screening, visualized by using the z-score. Activities against ASPC1 and resting PBMC were >10 $\mu$M. The zero value represents the mean concentration required to inhibit 50% of the growth for all cell lines ($GI_{50}$). The relative difference in the $GI_{50}$ value expressed as the z-score is represented by the horizontal bars. A positive z-score means that it is less sensitive to **33c** treatment; a negative z-score means that it is more sensitive to **33c** treatment. (B) Box-and-whisker diagram.

**Cell Panel Screen.** Cellular screening in combination with biochemical data can provide the rationale for optimization cycles and can be essential for understanding the specificity of compound action. Therefore, we explored the potencies of **28e**, **33b**, and **33c** against a broad range (83) of solid tumor cell lines.[49] The concept of the mean graph introduced by NCI permits visualization of a cell activity parameter for a given anticancer drug in all cells.[50] Our study included more cell lines (83 vs 60) and a broader spectrum of therapeutic indications (17 vs 7) than in NCI. We additionally prolonged compound treatment to 72 h to ensure the detection of effects even in slowly proliferating cell lines. In addition, resting peripheral blood mononuclear cells[51] (PBMC) were included into the screening. After treatment with test compounds, cell proliferation was determined by means of sulforhodamine B (SRB) staining.

The results obtained with this panel of cell lines further confirmed the high potency of **28e** (18−35 nM; see Supporting Information for details), **33b** (6−10 nM; see Supporting Information for details), and **33c** (1.8−2.7 nM, Table 4 and Figure 1 A,B), with all values referring to the eight most sensitive cell lines. The most sensitive and resistant cell lines were visualized either by using a box-plot graph (Figure 1B) or by selecting the 8 most and least sensitive cell lines using the z-score for each agent. The values are plotted as horizontal bars from the zero value, which represents the mean concentration required to inhibit 50% of the growth for all cell lines ($GI_{50}$). Each bar, therefore, represents the relative activity of the compound in the given cell lines deviating from the mean in all cell lines.

In spite of differences in absolute activities, the activity profiles of **28e** and **33b** were very similar (Pearson coefficient similarity of $r = 0.91$). Comparison of these activity profiles to the internal database identified similarities to a set of different tubulin inhibitors, such as 10-[(3-hydroxy-4-methoxy-benzylidene)]-9(10*H*)-anthracenone[17] (**6**, $r = 0.91$), combretastatin A-4[13] ($r = 0.86$), and 2-methoxyestradiol[18] (**7**, $r = 0.82$). In contrast, the similarity of **33c** to **33b** and **28e**, as well as to the tubulin inhibitors, was less significant (<0.76). Interestingly, for **33c**, no significant correlation could be observed to the "classical" tubulin inihibitors colchicine or vinblastine. Another difference was observed in activity distribution of these agents. Figure 1 demonstrates activities for


dx.doi.org/10.1021/jm200436t |*J. Med. Chem.* 2011, 54, 4247–4263

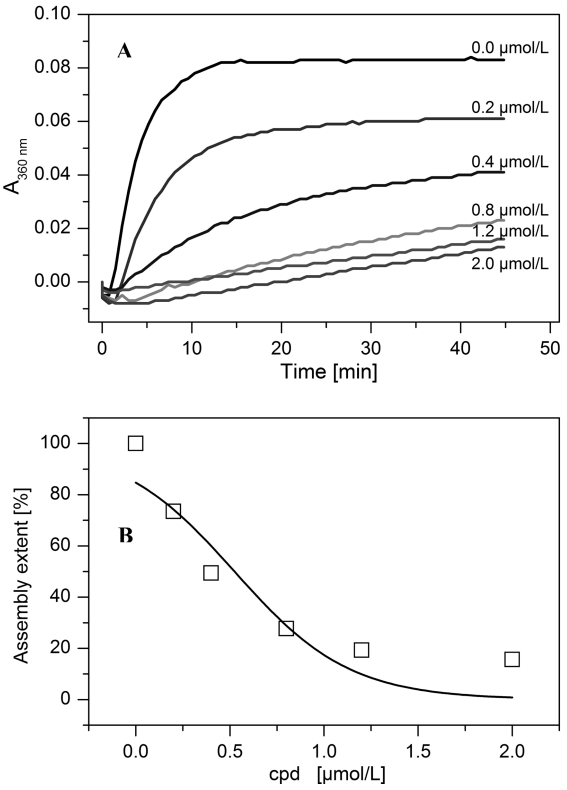


**Figure 2.** (A) Inhibition of in vitro polymerization of tubulin (in total 1.2 mg/mL protein; ~85% tubulin plus ~15% microtubule-associated proteins) at 37 °C by various concentrations of **33c**; turbidity was recorded at 360 nm. The steady-state tubulin assembly level in the absence of inhibitor was set at 100%. (B) $IC_{50}$ values were determined by sigmoidal fitting of the plot of the steady state levels of tubulin assembly (taken after 45 min) against drug concentration and represent the concentration for 50% inhibition of the maximum tubulin polymerization level.

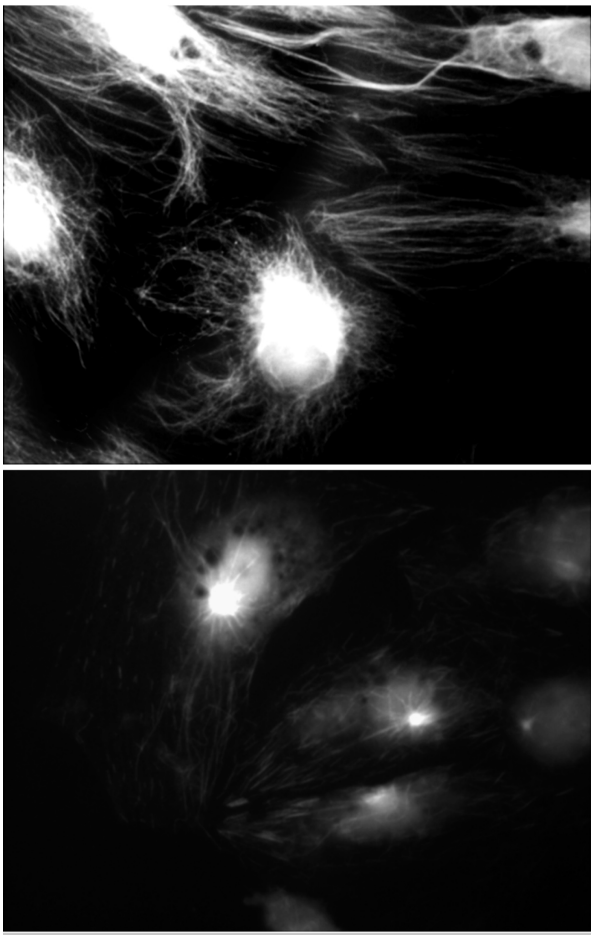

**Figure 3.** Effect of **28e** on cellular microtubules. Immunofluorescence images of PtK2 cells labeled with Cy3-antitubulin antibody. Top, cells incubated for 1 h in 2% DMSO; bottom, cells incubated for 1 h in 5 $\mu$M **28e**/2% DMSO.

**33c** within the range of 2 nM for the most sensitive cell lines to 8 $\mu$M for resistant cell lines (Table 4 and Figure 1). It is worth mentioning that the activity of **28e** in the most resistant cell lines (see Supporting Information) was in the same range as that for **33c**, whereas its potency in the most sensitive cell line was an order of magnitude less than that for **33c**.

Compounds **33b** and **33c** showed high potencies with cancer cell lines originating from the skin and brain showing above-average sensitivity (negative z-scores, see Supporting Information for details).

The human osteosarcoma cell line MG-63, human neuroblastoma SKNAS and SK-N-SH cells, and human bladder carcinoma cell line 5637 were found to be among the most responsive cell lines against **28e**, **33b**, and **33c**. No activity was shown in resting PBMC, suggesting that these agents may act preferably on proliferating cells.

**In Vitro Tubulin Polymerization Assays.** To explore whether the growth inhibitory effect of our compounds is correlated with an interaction with the tubulin system, we measured their effect on the polymerization of tubulin in a cell-free system. Their activity was compared with that of the reference anti-tubulin compounds colchicine, podophyllotoxin, nocodazole, and vinblastine (Table 1). In the presence of GTP and $Mg^{2+}$, $\alpha\beta$-tubulin is known to be able to self-assemble (polymerize) in vitro into microtubules at physiological temperature (37 °C), accompanied by changes of light scattering (turbidity). The turbidity curves, usually obtained at 340−360 nm, reveal a sigmoid behavior with a plateau level reached after 20−30 min at the conditions realized in this study. Inhibition of tubulin polymerization is reflected by a decreased level of steady state turbidity in a dose-dependent manner as exemplified for **33c** (Figure 2A).

The phenothiazine derivative **14b** ($IC_{50}$ ITP 0.87 $\mu$M) inhibited tubulin polymerization at submicromolar concentration, whereas **9e** and **17a** displayed inhibitory activities comparable to that of colchicine (Table 1). The phenothiazines **9b**, **16a**, **18g**, **19b**, **19c**, and **19i** were moderate inhibitors of tubulin polymerization with $IC_{50}$ values in the range of 2−3 $\mu$M, somewhat less active than colchicine (ITP $IC_{50}$ 1.4 $\mu$M). It is striking to note that potencies of the phenothiazines and the corresponding sulfones were comparable, whereas the sulfoxides **18b**,**18c**, **18e**, **18h**, and **18i** were more or less ineffective tubulin polymerization inhibitors ($IC_{50} \geq 10\ \mu$M). These low potencies, particularly in the case of **18b**, **18e**, and **18h** were not consistent with our findings that these compounds were good inhibitors of K562 tumor cell growth. On the one hand, these compounds might exert their antiproliferative action by an alternative mechanism. On the other hand, as already pointed out, formation of the sulfones under the conditions of the cellular assay cannot be excluded.

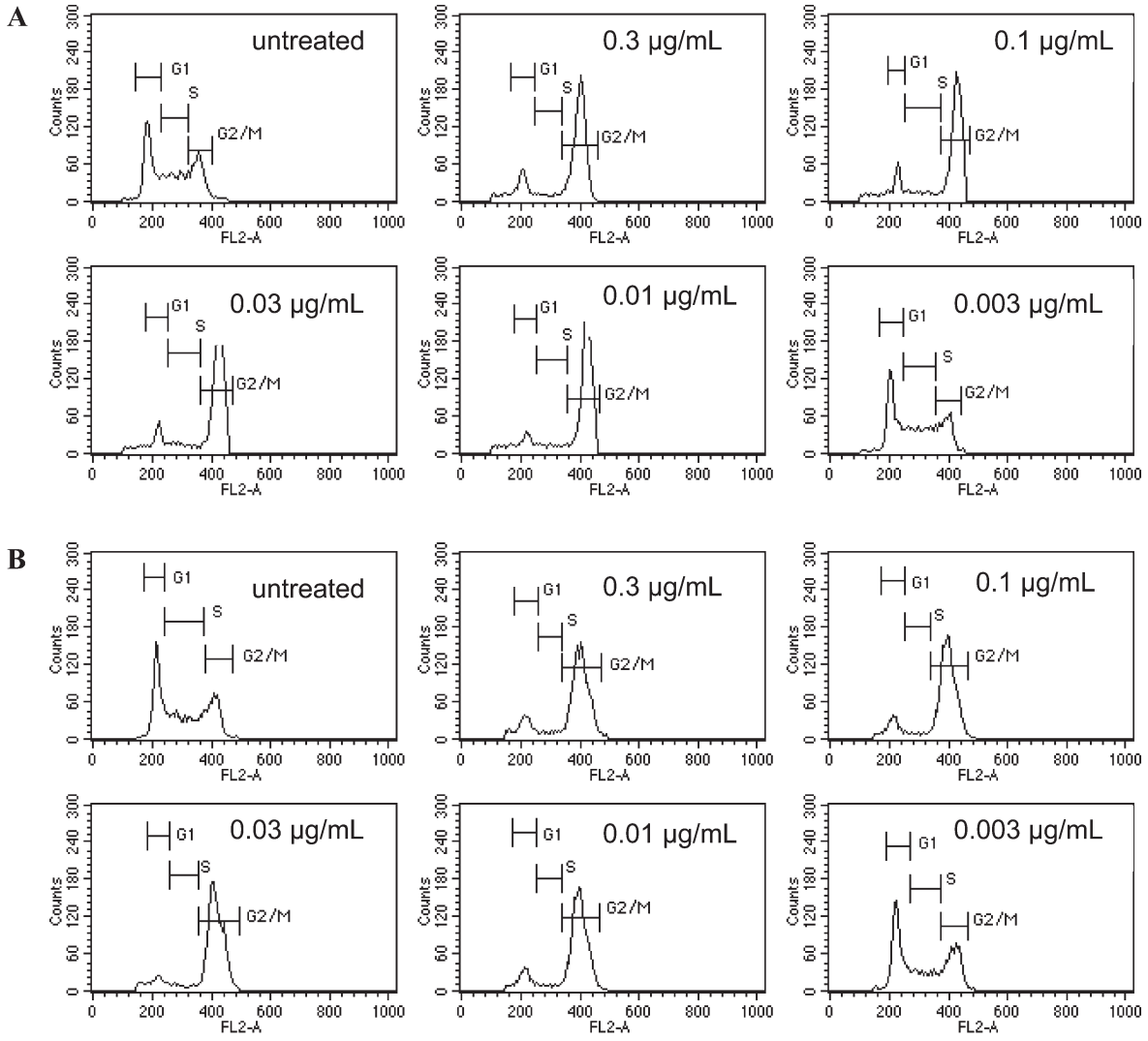


**Figure 4.** Induction of cell cycle arrest by **33b**. Cell cycle distribution of K562 cells showing the effect of 24 h-treatment with **33b** (A) and colchicine (B) (24 h assay). K562 cells were untreated, treated with different concentrations of **33b** (A) or colchicine (B). After treatment, the cells were collected and cell cycle distribution was measured by flow cytometry with FACSCalibur (Becton Dickinson), Software CellQuest Pro, version 5.2.

In the phenoxazine series, inhibition of tubulin polymerization generally correlated well with drug-induced growth inhibition. The compounds with the highest antiproliferative activity (**10a**, **28e**, **33b**, and **33c**) were found also among the strongest inhibitors of tubulin polymerization. Eight phenoxazines (**28a**, **28b**, **28e**, **28g**, **28m**, **29a**, **33b**, and **33c**) proved to be exceptionally strong inhibitors of tubulin polymerization ($IC_{50} \leq 1\ \mu M$). Paralleling the results from the antiproliferative studies, the 4-methoxy as well as 3-hydroxy-4-methoxy phenyl were crucial moieties for the inhibition of tubulin polymerization. Four compounds (**10a**, **28c**, **28h**, and **33a**) displayed nearly the same activity and were as active as colchicine with $IC_{50}$ values in the range of 1 $\mu$M. Notably, the phenoxazines **28g**, **28k**, and even **28n**, which was found to be nearly inactive in the K562 assay, showed good to moderate tubulin inhibiting activity. This is probably due to the fact that the tubulin polymerization assay is not a cell-based assay, thus differing in a number of important issues, such as tubulin concentration present within the cells or possible effects of regulatory proteins expressed in the cell but being absent in the tubulin assay. Other important aspects could be differences in cell permeability of the various compounds or reduced stability of the compounds in the cell supernatant compared to the cell-free assay.

To study the effect on the microtubule system on the cellular level, PtK2 cells were exposed for 1 h to 5 $\mu$M of phenothiazine **28e**, added to RPMI medium. Immunofluorescence microscopy revealed that the complex microtubule network has been destroyed, whereas in the control preparation, treated with the solvent (DMSO) only, the intracellular network of microtubules was seen to be organized in large bundles irradiating from the cell center (Figure 3).

Only a few single short microtubules remained after **28e** action (Figure 3). The effect of **28e** on the PtK2 microtubule system was qualitatively and quantitatively comparable to that of 5 $\mu$M colchicine (data not shown).

**Effect on Cell-Cycle Progression.** By targeting mitotic spindle formation, microtubule-binding agents should alter cell cycle parameters with preferential G2/M blockade. As a consequence, mitosis would be blocked at the transition from metaphase to anaphase, thereby affecting chromosome segregation.[52,53]

Cell cycle arrest is a typical feature for the majority of antimitotic agents. Using a K562 cell-based assay, we investigated the highly active compounds **33b** and **33c** for effects on the cell cycle. The cells were exposed to test compounds in different concentrations, and the percentage of cells in G2/M phase after 24 h was monitored. Phenoxazine-derived amides **33b** and **33c** blocked mitosis through an arrest of cells in the G2/M phase, as illustrated in typical histograms (Figure 4; see Supporting Information for **33c**).

Both compounds effectively arrested cell cycle progression at concentrations down to 30 nM (Table 4), i.e., they are nearly as active as colchicine. This result indicates that from the series of compounds represented in this article at least the phenoxazine-derived amides **33b** and **33c** can be classified as antimitotic drugs with high activity.

## CONCLUSIONS

Synthesis and structure−activity relationship studies for a new class of synthetic inhibitors of tubulin polymerization, based on a phenothiazine and phenoxazine molecular skeleton, were carried out. These compounds (e.g., **9e**, **10a**, **33b**, and **33c**) represent novel and highly potent inhibitors of cancer cell growth and tubulin polymerization. Replacement of sulfur in the phenothiazine ring with oxygen in general increased the antiproliferative activity. Furthermore, the SAR information revealed that the introduction of a cyano group into the 3-position of the phenoxazine moiety substantially improved the antiproliferative potency compared with that of the unsubstituted analogues. The most promising phenoxazines **33b** and **33c** inhibited tubulin polymerization more efficiently than the reference compound colchicine and inhibited the growth of multiple cancer cell lines with $IC_{50}$ values in the range of 2−15 nM.

A *p*-methoxy substitution pattern or a isovanillic partial structure in the terminal phenyl ring was proved to be essential for both potent inhibition of tumor cell proliferation and inhibition of tubulin polymerization. The observed antiproliferative effects are most probably due to the interaction with tubulin as those compounds with the greatest inhibitory effects on cell growth strongly inhibited tubulin polymerization. Potent induction of G2/M arrest, similar to that of colchicine, was demonstrated for the most active phenoxazines **33b** and **33c**. Given the relative ease of synthesis and due to their high in vitro antitumor activities, we envision that compounds of this structural class are attractive for further structural modifications. Moreover, our findings are expected to provide useful information for the design of novel antitumor agents.

Further structure−activity studies in the series of phenothiazine- and phenoxazine-based tubulin polymerization inhibitors are in progress, and results from other modifications will be reported in due course.

## EXPERIMENTAL SECTION

Melting points were determined with a Kofler melting point apparatus and are uncorrected. Spectra were obtained as follows: $^1$H NMR spectra were recorded with Varian Gemini 2000 or Varian Mercury 400 plus (400 MHz) spectrometers operating at 300 and 400 MHz, respectively. NMR signals were referenced to TMS ($\delta$ = 0 ppm) or solvent signals and recalculated relative to TMS. Fourier-transform IR spectra were recorded on a Bio-Rad laboratories Typ FTS 135 spectrometer, and analysis was performed with WIN-IR Foundation software. Mass spectra were obtained on Finnigan GCQ and LCQ apparatuses applying electron beam ionization (EI) and electrospray ionization (ESI). The atmospheric pressure chemical ionization (APCI) method was performed with a microTOF-QII apparatus (Bruker). The purity of all target compounds was determined either by elemental analyses or by reversed phase HPLC at 254 nm. Compound purity for all target compounds is ≥95%. Elemental analyses were performed at Münster Microanalysis Laboratory, using a Vario EL elemental analyzer from Elementar Analysensysteme GmbH Hanau, and all values were within ±0.4% of the calculated composition. The HPLC system applied a C18 phase (Nucleosil, 3 $\mu$m, 4.0 × 125 mm, CS-Chromatographie Service GmbH, Langerwehe, Germany) eluting the compounds with an acetonitrile/$H_2O$ gradient at a flow rate of 0.40 mL/min. All organic solvents were appropriately dried or purified prior to use. Acid chlorides were obtained from commercial sources or prepared to literature protocols. Purification by chromatography refers to column chromatography on silica gel (Macherey-Nagel, 70−230 mesh). In most cases, the concentrated pure fractions obtained by chromatography using the indicated eluants were treated with a small amount of hexane to induce precipitation. All new compounds displayed $^1$H NMR and MS spectra consistent with the assigned structure. Yields have not been optimized. Analytical TLC was done on Merck silica 60 $F_{254}$ alumina coated plates (E. Merck, Darmstadt). Chromatography refers to column chromatography using Acros 60−200 mesh silica gel.

**10-Benzoyl-10*H*-phenothiazine (9a).**[33,54] See Supporting Information for details.

**10-4-Methoxybenzoyl)-10*H*-phenothiazine (9b).**[33,54] A solution containing **9** (4.04 g, 20.3 mmol) and 4-methoxybenzoyl chloride (4.14 g, 24.35 mmol) in toluene (80 mL) was refluxed with stirring until all of **9** was consumed (TLC control). Then, the reaction mixture was cooled and washed successively with aqueous sodium bicarbonate 20% (3 × 15 mL), hydrochloric acid 6% (3 × 50 mL), and finally with water (2 × 50 mL). The solution was dried ($Na_2SO_4$) and filtered, and the solvent was evaporated. The crude product was purified by chromatography ($CH_2Cl_2$/hexane, 9:1) to give **9b** as a white powder (5.88 g, 87%). mp 170−175 °C (lit.[33] 173−174 °C). FTIR 1654 cm$^{-1}$; $^1$H NMR (DMSO, 400 MHz, 300K) $\delta$ 7.92 (dd, $J$ = 6.9, $J$ = 2.2 Hz, 2H), 7.75 (dd, $J$ = 7.8, $J$ = 1.4 Hz, 2H), 7.55−7.42 (m, 6H), 6.84 (d, $J$ = 8.9 Hz, 2H), 3.72 (s, 3H); MS (ESI) calcd for $C_{20}H_{15}NO_2S$ $[M + Na]^+$ 356.07; found, 356.07; Anal. $C_{20}H_{15}NO_2S$.

**10-(3,4,5-Trimethoxybenzoyl)-10*H*-phenothiazine (9c).**[55] See Supporting Information for details.

**10-(3-(Benzyloxy)-4-methoxybenzoyl)-10*H*-phenothiazine (9d).** See Supporting Information for details.

**10-(3-Hydroxy-4-methoxybenzoyl)-10*H*-phenothiazine (9e).** $AlCl_3$ (0.36 g, 2.7 mmol) was added at room temperature to a solution of **9d** (0.42 g, 0.96 mmol) in $CH_2Cl_2$ (40 mL). After complete conversion, as indicated by TLC, the solution was poured into water and extracted with $CH_2Cl_2$ (3 × 50 mL). The combined organic phases were dried over $Na_2SO_4$. Evaporation of the solvent under reduced pressure provided a crude solid, which was purified by silica gel chromatography (ethyl acetate/$CH_2Cl_2$ 1:4) to afford **9e** as a white powder (0.30 g, 90%). mp 208 209 °C; FTIR 1630 cm$^{-1}$; $^1$H NMR (DMSO-$d_6$, 400 MHz, 300K) $\delta$ 9.19 (s, 1H), 7.55 (m, 2H), 7.44 (m, 2H), 7.27−7.21 (m, 4H), 6.80 (d, $J$ = 2.0 Hz, 1H), 6.75 (d, $J$ = 8.4 Hz, 1H), 6.68 (dd, $J$ = 8.3, 2.0 Hz, 1H), 3.70 (s, 3H); MS (APCI) calcd for $C_{20}H_{15}NO_3S$ $[M + H]^+$ 350.08; found, 350.08. Anal. $C_{20}H_{15}NO_3S$.

**10-(4-Methoxybenzoyl)-10*H*-phenoxazine (10a).** See Supporting Information for details.

**10-(4-Methoxyphenylacetyl)-10*H*-phenoxazine (10b).** See Supporting Information for details.

**10-Benzoyl-2-chloro-10*H*-phenothiazine (14a).** See Supporting Information for details.

**2-Chloro-[10-(4-methoxybenzoyl)]-10*H*-phenothiazine (14b).** See Supporting Information for details.

**2-Chloro-10-(3,4,5-trimethoxybenzoyl)-10*H*-phenothiazine (14c).** See Supporting Information for details.

**2-Chloro-[10-(4-methoxyphenylacetyl)]-10*H*-phenothiazine (14d).** See Supporting Information for details.

**2-(Trifluoromethyl)-10-(2-methoxybenzoyl)-10*H*-phenothiazine (15a).** See Supporting Information for details.

**2-Methoxy-10*H*-phenothiazine (16).**[41] The title compound was prepared according to the literature protocol.

**2-Methoxy-10-(4-methoxybenzoyl)-10*H*-phenothiazine (16a).** See Supporting Information for details.

**10-(2-Methoxybenzoyl)-2-(methylthio)-10*H*-phenothiazine (17a).** See Supporting Information for details.

**10-Benzoyl-10*H*-phenothiazine-5-oxide (18a).** The title compound was prepared from **9a** (0.5 g, 1.7 mmol) and *m*CPBA, 70−75% (0.29 g, 1.7 mmol) in $CH_2Cl_2$ (20 mL). The mixture was stirred at room temperature for 12 h and then concentrated in vacuo. Purification of the residue by chromatography (ethyl acetate/$CH_2Cl_2$ 1:9) afforded **18a** as a white powder (0.36 g, 66%). mp 176−181 °C; FTIR 1673 $cm^{-1}$; $^1H$ NMR (DMSO-$d_6$, 400 MHz, 300 K) $\delta$ 7.96−7.86 (m, 2H), 7.71 (m, 2H), 7.55−7.44 (m, 6H), 7.39 (t, $J$ = 7.4 Hz, 1H), 7.30 (t, $J$ = 7.5 Hz, 2H); MS (ESI) calcd for $C_{19}H_{13}NO_2S$ $[M + Na]^+$ 342.06; found, 342.06. Anal. ($C_{19}H_{13}NO_2S$) C, H, N.

**10-(4-Methoxybenzoyl)-10*H*-phenothiazine-5-oxide (18b).** See Supporting Information for details.

**10-(3,4,5-Trimethoxybenzoyl)-10*H*-phenothiazine-5-oxide (18c).** See Supporting Information for details.

**10-(3-(Benzyloxy)-4-methoxybenzoyl)-10*H*-phenothiazine-5-oxide (18d).** See Supporting Information for details.

**10-(3-Hydroxy-4-methoxybenzoyl)-10*H*-phenothiazine-5-oxide (18e).** See Supporting Information for details.

**2-Chloro-10-benzoyl-10*H*-phenothiazine-5-oxide (18f).** See Supporting Information for details.

**2-Chloro-10-(4-methoxybenzoyl)-10*H*-phenothiazine-5-oxide (18g).** See Supporting Information for details.

**2-Chloro-10-(3,4,5-trimethoxybenzoyl)-10*H*-phenothiazine-5-oxide (18h).** See Supporting Information for details.

**2-Methoxy-10-(4-methoxybenzoyl)-10*H*-phenothiazine-5-oxide (18i).** See Supporting Information for details.

**10-Benzoyl-10*H*-phenothiazine-5,5-dioxide (19a).** A solution of **9a** (1.2 g, 3.95 mmol) and 30% $H_2O_2$(10 mL) in glacial acetic acid (30 mL) was stirred and refluxed for 2 h. The solution was then cooled, poured into water, and extracted with $CH_2Cl_2$ (3 × 100 mL). The combined organic layers were dried over $Na_2SO_4$ and concentrated under reduced pressure. Chromatography of the residue (ethyl acetate/$CH_2Cl_2$ 1:9) afforded **19a** as a white powder (0.73 g, 55%). mp 253−257 °C; FTIR 1681 $cm^{-1}$; $^1H$ NMR (DMSO-$d_6$, 300 MHz, 300 K) $\delta$ 8.09−8.00 (m, 2H), 7.85−7.77 (m, 2H), 7.59 (m, 4H), 7.51−7.29 (m, 5H); MS (ESI) calcd for $C_{19}H_{13}NO_3S$ $[M + Na]^+$ 358.05; found, 358.05. Anal. ($C_{19}H_{13}NO_3S$) C, H, N.

**10-(4-Methoxybenzoyl)-10*H*-phenothiazine-5,5-dioxide (19b).** See Supporting Information for details.

**10-(3,4,5-Trimethoxybenzoyl)-10*H*-phenothiazine-5,5-dioxide (19c).** See Supporting Information for details.

**10-(3-(Benzyloxy)-4-methoxybenzoyl)-10*H*-phenothiazine-5,5-dioxide (19d).** See Supporting Information for details.

**10-(3-Hydroxy-4-methoxybenzoyl)-10*H*-phenothiazine-5,5-dioxide (19e).** See Supporting Information for details.

**10-Benzoyl-2-chloro-10*H*-phenothiazine-5,5-dioxide (19f).** See Supporting Information for details.

**2-Chloro-10-(4-methoxybenzoyl)-10*H*-phenothiazine-5,5-dioxide (19g).** See Supporting Information for details.

**2-Chloro-10-(3,4,5-trimethoxybenzoyl)-10*H*-phenothiazine-5,5-dioxide (19h).** See Supporting Information for details.

**2-Methoxy-10-(4-methoxybenzoyl)-10*H*-phenothiazine-5,5-dioxide (19i).** See Supporting Information for details.

**1-(2-Bromophenoxy)-4-chloro-2-nitro-benzene (20).**[38,56] The title compound was prepared according to the literature protocol.

**2-Bromo-4-chloro-1-(4-chloro-2-nitrophenoxy)-benzene (21).** See Supporting Information for details.

**2-(2-Bromophenoxy)-5-chloro-aniline (22).**[38] The title compound was prepared according to the literature protocol.

**2-(2-Bromo-4-chlorophenoxy)-5-chloro-aniline (23).** See Supporting Information for details.

**N-[2-(2-bromophenoxy)-5-chlorophenyl]-formamide (24).**[38] The title compound was prepared according to the literature protocol.

***N*-(2-(2-bromo-4-chlorophenoxy)-5-chlorophenyl)formamide (25).** See Supporting Information related to **27** for details.

**2-Chloro-10*H*-phenoxazine-10-carboxaldehyde (26).**[38,56] The title compound was prepared according to the literature protocol.

**2,8-Dichloro-10*H*-phenoxazine-10-carboxaldehyde (27).** See Supporting Information for details.

**2-Chloro-10*H*-phenoxazine (28).**[38,56] The title compound was prepared according to the literature protocol.

**2-Chloro-10-(4-methoxybenzoyl)-10*H*-phenoxazine (28a).** 4-Methoxybenzoyl chloride (4 mmol, 0.68 g) was added to a suspension of 2-chlorophenoxazine **28** (4 mmol, 0.87 g) in toluene (50 mL). The mixture was heated under reflux until the reaction was complete (TLC control, $SiO_2$, and ethyl acetate/petrol ether 1:1). Then, the solvent was removed in vacuo, and the residue was purified by chromatography (ethyl acetate/petrol ether 1:1) to afford **28a** (0.79 g, 56%) as a white powder. mp 148−149 °C; FTIR 1658 $cm^{-1}$; $^1H$ NMR ($CDCl_3$, 400 MHz, 300 K) $\delta$ 7.76 (d, 1H, $J$ = 2.35 Hz), 7.41 (d, 2H, $J$ = 8.61 Hz), 7.12−7.02 (m, 5H), 6.90−6.87 (m, 1H), 6.78 (d, 2H, $J$ = 9.00 Hz) 3.81 (s, 3H); MS (EI, 70 eV) $m/z$ (%) 352.94 (2.64), 351.88 (2.60), 350.91 (9.76), 135.11 (100). Anal. ($C_{20}H_{14}ClNO_3$) C, H, N.

**2-Chloro-10-(3-methoxybenzoyl)-10*H*-phenoxazine (28b).** See Supporting Information for details.

**2-Chloro-[10-(4-methoxyphenylacetyl)]-10*H*-phenoxazine (28c).** See Supporting Information for details.

**2-Chloro-[10-(3-benzyloxy-4-methoxybenzoyl)]-10*H*-phenoxazine (28d).** See Supporting Information for details.

**2-Chloro-[10-(3-hydroxy-4-methoxybenzoyl)]-10*H*-phenoxazine (28e).** $AlCl_3$ (0.27 g, 2 mmol) was added to a solution of **28d** (1 mmol, 0.46 g) in 1,2-dichloroethane (20 mL) at 0 °C, and the mixture was stirred until the reaction was completed. The solution was then poured into water (200 mL) and extracted with $CH_2Cl_2$ (3 × 30 mL). The combined organic layers were washed with water (2 × 50 mL) and dried over anhydrous $Na_2SO_4$. The solvent was then removed in vacuo, and the residue was purified by chromatography on silica gel ($CH_2Cl_2$) to give **28e** (0.11 g, 30%) as a white powder. mp 145−147 °C; FTIR 3352, 1648 $cm^{-1}$; $^1H$ NMR ($CDCl_3$, 400 MHz, 300 K) 7.74 (d, 1H, $J$ = 2.34 Hz), 7.12−7.09 (m, 4H), 7.05 (d, 1H, 2.35 Hz), 7.03 (d, 1H, $J_o$ = 8.61 Hz), 6.98−6.96 (m, 1H), 6.91−6.86 (m, 1H), 6.71 (d, 1H, $J$ = 8.61 Hz), 5.61 (s, 1H), 3.89 (s, 3H). Purity (HPLC): 97.4%.

**2-Chloro-[10-(4-benzyloxy-3,5-dimethoxybenzoyl)]-10*H*-phenoxazine (28f).** See Supporting Information for details.

**2-Chloro-[10-(3,5-dimethoxy-4-hydroxybenzoyl)]-10*H*-phenoxazine (28g).** See Supporting Information for details.

**2-Chloro-[10-(3,4-methylenedioxybenzoyl)]-10*H*-phenoxazine (28h).** See Supporting Information for details.

**2-Chloro-[10-(3,4,5-trimethoxybenzoyl)]-10*H*-phenoxazine (28i).** See Supporting Information for details.

**2-Chloro-[10-(4-trifluoromethylbenzoyl)]-10*H*-phenoxazine (28j).** See Supporting Information for details.

**2-Chloro-[10-(4-chlorobenzoyl)]-10*H*-phenoxazine (28k).** See Supporting Information for details.

**2-Chloro-[10-(4-bromobenzoyl)]-10*H*-phenoxazine (28l).** See Supporting Information for details.

**2-Chloro-[10-(4-dimethylaminobenzoyl)]-10*H*-phenoxazine (28m).** See Supporting Information for details.

**2-Chloro-[10-(4-nitrobenzoyl)]-10*H*-phenoxazine (28n).** See Supporting Information for details.

**2-Chloro-10-acetyl-10*H*-phenoxazine (28o).** See Supporting Information for details.

**2,8-Dichloro-10*H*-phenoxazine (29).** See Supporting Information for details.

**2,8-Dichloro-[10-(4-methoxybenzoyl)]-10*H*-phenoxazine (29a).** See Supporting Information for details.

**10*H*-Phenoxazine-2-carbonitrile (32).** The title compound was prepared according to a literature protocol;[45] mp 213−214 °C (lit.[45] 212−214 °C).

**10-(4-Methoxybenzoyl)-10*H*-phenoxazine-2-carbonitrile (32a).** See Supporting Information for details.

**10*H*-phenoxazine-3-carbonitrile (33).**[45] A mixture of 2-aminophenol (1.96 g, 18.0 mmol), dissolved in DMF (30 mL), potassium carbonate (5.0 g), and toluene (20 mL) was heated under reflux ($N_2$, Dean−Stark). It was then cooled to 80 °C, and 3,4-difluorobenzonitrile (2.50 g, 17.97 mmol) was added. The mixture was again heated under reflux for 4 h. Thereafter, toluene was distilled off and replaced with DMF. The mixture was then heated at 150 °C for 2 h (TLC control). After cooling to room temperature, NaOH (2N, 100 mL) was added. The mixture was then extracted with $CH_2Cl_2$ (3 × 50 mL). The combined organic layers were washed with water, dried ($Na_2SO_4$), and concentrated under reduced pressure. Purification of the residue by chromatography ($CH_2Cl_2$) gave **33** as a yellow crystalline solid (2.77 g, 74%). mp 202−203 °C (lit.[45] 198−199 °C).

**10-Benzoyl-10*H*-phenoxazine-3-carbonitrile (33a).** See Supporting Information for details.

**10-(4-Methoxybenzoyl)-10*H*-phenoxazine-3-carbonitrile (33b).** A mixture of **33** (0.21 g, 1 mmol) and 4-methoxybenzoyl chloride (0.17 g, 1 mmol) in toluene (15 mL) was stirred and heated under reflux (oil bath, 130 °C). After 5 h (TLC control), the mixture was cooled to room temperature, and the solvent was evaporated in vacuo. Purification of the residue by chromatography ($CH_2Cl_2$) afforded **33b** as white crystals (0.10 g, 30%). mp 184−185 °C; FTIR 2228, 1672 $cm^{-1}$; $^1H$ NMR ($CDCl_3$, 300 MHz, 300 K) $\delta$ 7.70 (d, 1H, $J$ = 8.4 Hz), 7.40−7.34 (m, 2H), 7.31 (d, 1H, $J$ = 1.8 Hz), 7.23 (dd, 1H, $J$ = 8.4 Hz, $J$ = 1.9 Hz), 7.11−7.03 (m, 3H), 6.89−6.83 (m, 1H), 6.75−6.69 (m, 2H), 3,74 (s, 3H). Anal. $C_{21}H_{14}N_2O_3$, MS (ESI) calcd for $C_{21}H_{14}N_2O_3$ $[M + Na]^+$ 365.09; found, 365.09. Anal. $C_{21}H_{14}N_2O_3$.

**10-(3-Hydroxy-4-methoxybenzoyl)-10*H*-phenoxazine-3-carbonitrile (33c).** A mixture of 3-benzyloxy-4-methoxybenzoic acid[57] (0.26 g, 1 mmol) and oxalyl chloride (14.55 g, 115.63 mmol) was stirred in an ice bath (0 °C) until the solution turned clear (1 h). Then, excess oxalyl dichloride was removed under reduced pressure. 10*H*-Phenoxazine-3-carbonitrile (**33**, 0.21 g, 1 mmol) was added, and the mixture was heated under reflux in pyridine. After the reaction was completed (TLC control, 6 h), the mixture was poured into ice water, acidified with HCl (100 mL, 4 N) and extracted with $CH_2Cl_2$ (3 × 50 mL). The combined organic layers were washed with water (2 × 50 mL) and dried over anhydrous $Na_2SO_4$, and the solvent was removed in vacuo. The crude residue (0.32 g, 0.9 mmol crude product) was suitable for use without purification and dissolved in $CH_2Cl_2$ at 0 °C. $AlCl_3$ (0.60 g, 4.5 mmol) was added, and the color turned from yellow to dark red. After the reaction was completed (4 h, TLC control), water was added, and the mixture was extracted with $CH_2Cl_2$ (3 × 50 mL). The combined organic layers were washed with water (2 × 50 mL) and dried over anhydrous $Na_2SO_4$, and the solvent was removed in vacuo. Purification of the organic phase by chromatography (ethyl acetate/petroleum ether 3:7) afforded **33c** as a beige powder (0.26 g, 73%). mp 173−175 °C; FTIR 3393, 2235, 1675 $cm^{-1}$; $^1H$ NMR ($CDCl_3$, 300 MHz, 300 K) $\delta$ 7.67 (d, 1H, $J$ = 8.4 Hz), 7.31 (d, 1H, $J$ = 1.8 Hz), 7.22 (dd, 1H, $J$ = 8.4, 1.9 Hz), 7.17−7.12 (m, 1H), 7.11−7.01 (m, 3H), 6.96−6.84 (m, 2H), 6.65 (d, 1H, $J$ = 8.4 Hz), 5.56 (s, 1H), 3.83 (s, 3H). Anal. $C_{21}H_{14}N_2O_4$, MS (APCI) calcd for $C_{21}H_{14}N_2O_4$ $[M + H]^+$ 359.10; found, 359.11. Anal. $C_{21}H_{14}N_2O_4$.

**10-(4-Chlorobenzoyl)-10*H*-phenoxazine-3-carbonitrile (33d).** See Supporting Information for details.

**10*H*-Phenoxazine-1-carbonitrile (34).** The title compound was prepared according to a literature protocol.[45] mp 186 °C (lit.[45] 182−184 °C).

**10-(4-Methoxybenzoyl)-10*H*-phenoxazine-1-carbonitrile (34a).** See Supporting Information for details.

**2-(2-Chloro-phenoxazin-10-yl)-1-(4-methoxy-phenyl)-ethanone (35).** 2-Chlorphenoxazine **28** (0.65 g, 3 mmol) and TBAB (0.1 g, 0.3 mmol) were suspended in a mixture of NaOH 50% (5 mL), THF (2 mL) and water (2 mL). Then, a solution of 2-bromo-1-(4-methoxyphenyl)ethanone (1.37 g, 6 mmol) in THF (5 mL) was added in one portion. The reaction mixture was then stirred at room temperature for 1 h, poured into water (400 mL), acidified with 6 N HCl, and extracted with $CH_2Cl_2$ (3 × 30 mL). The combined $CH_2Cl_2$ extracts were washed, dried over $Na_2SO_4$, and then evaporated. Purification by chromatography ($CH_2Cl_2$) gave **35** as a white solid (0.71 g, 63%). mp 179 °C; FTIR 1677 $cm^{-1}$; $^1H$ NMR ($CDCl_3$, 400 MHz, 300 K) 8.05 (d, 2H, $J$ = 9.0 Hz), 7.03 (d, 2H, $J$ = 9.0 Hz), 6.74−6.70 (m, 3H), 6.63−6.60 (m, 2H), 6.19−6.14 (m, 2H), 4.90 (s, 2H), 3.92 (s, 3H); MS (APCI) calcd for $C_{21}H_{16}ClNO_3$ $[M + H]^+$ 365.08; found, 365.08. Anal. ($C_{21}H_{16}ClNO_3$) C, H, N.

**Biological Assay Methods.** *Cells and Culture Conditions.* Human chronic myelogenous K562 leukemia cells were obtained from DSMZ, Braunschweig, Germany, and cultured at 37 °C under 5% $CO_2$ in RPMI 1640 medium (Gibco) containing 10% fetal bovine serum (FBS, Biochrom KG), streptomycin (0.1 mg/mL), penicillin G (100 units/mL), and L-glutamine (30 mg/L). Cell line SF268 (central nerval system carcinoma) was obtained from NCI. The human tumor cell lines SKOV3 (ovarian adenocarcinoma), NCI-H460 (lung), BT549 (breast carcinoma), 451LU (lung), SW480 (colon adenocarcinoma), COLO-205 (colon), and DLD-1 (colon adenocarcinoma) were obtained from ATCC.

Screening of the agents in a panel of 83 cell lines from solid tumors by means of sulforhodamine B staining was performed by following the protocol described by DTP NCI (http://dtp.nci.nih.gov/branches/btb/ivclsp.html) and in more details specific to this study in Supporting Information.

*Assay of Cell Growth.* K562 cells were plated at 2 × $10^5$ cells/mL in 24 well dishes (Costar, Cambridge, MA). Untreated control wells were assigned a value of 100%. Test compounds were made soluble in DMSO/methanol 1:1, and control wells received equal volumes (0.5%) of vehicle alone. We demonstrated that 0.5% DMSO (final DMSO concentration in all samples including the controls) did not affect K562 cell growth. To each well, 5 $\mu$L of compound was added, and the final volume in the well was 500 $\mu$L. Cell numbers were counted with a Neubauer counting chamber (improved, double grid) after 48-h compound exposure. Each assay was prepared in triplicate, and the experiments were carried out three times. $IC_{50}$ values were obtained by nonlinear regression (GraphPad Prism) and represent the concentration at which cell growth was inhibited by 50%. The adjusted cell number was calculated as a percentage of the control, which was the number of cells in wells without the test compound.

*Cellular Viability Assay.* The AlamarBlue reagent is based on the dye Resazurin, which exhibits fluorescence change in the appropriate oxidation−reduction range relating to cellular metabolic reduction.[48] The increase of fluorescence at 590 nM is an indicator of cellular viability/cell number. The cells were seeded in the respective growth medium in 125 $\mu$L per 96 wells and were grown for 24 h at 37 °C/5%$CO_2$.

For dose−response analysis, 10 mM compound stocks in 100% DMSO were diluted in half logarithmic steps in cell medium. The final DMSO concentration in compound and control wells is adjusted to 0.316%. Twenty-five microliters of the respective compound dilutions are added per 96 wells. After 45 h of compound incubation at 37 °C/5% $CO_2$, 15 $\mu$L of the detection reagent AlamarBlue (AbD Serotec, cat. no. BUF012B) was added for an additional 3 h, and after a total of 48 h of compound incubation, the cellular metabolic activity was quantified by measurement of fluorescence at 590 nm. Nontreated cells and blank controls without cells are set as reference values. $IC_{50}$ values were obtained by nonlinear regression (GraphPad Prism).

*Isolation of MTP and In Vitro MT Assembly Assay by Turbidimetric Measurement.* Microtubule protein (MTP) consisting of 80 to 90% tubulin and 10 to 20% microtubule associated proteins (MAPs) was isolated from the porcine brain by two cycles of temperature-dependent disassembly (0 °C)/reassembly (37 °C), according to the described procedures.[58,59] Throughout the preparation, a buffer containing 20 mM PIPES (1,4-piperazine diethane sulfonic acid, pH 6.8), 80 mM NaCl, 0.5 mM $MgCl_2$, 1 mM ethylene bis-(oxyethylenenitrilo) tetraacetic acid, and 1 mM dithiothreitol was used. To start tubulin polymerization, stock MTP solutions were diluted with the preparation buffer to 1.2 mg/mL (corresponding to a final tubulin concentration of about 10 $\mu$mol/L) in glass cuvettes, guanosin-5′-triphosphate was added to 0.6 mM (final concentration), and the samples were transferred into a Cary 4E spectrophotometer (Varian Inc.), equipped with a temperature-controlled multichannel cuvette holder, adjusted to 37 °C. Turbidity, which increased as a result of tubulin polymerization,[60] was recorded at 360 nm over 45 min.

The test compounds were added from stock solutions made in DMSO. The final DMSO concentration was 1%. Control measurements were made with DMSO only. To quantify the drug activity, the turbidity signal after 45 min (plateau level, representing the assembly/disassembly steady state) was compared with that of the control samples. The $IC_{50}$ value is defined as the drug concentration that causes a 50% inhibition in relation to the assembly level without the drug.

*Flow Cytometric Analysis of Cell Cycle Status.* K562 cells ($2 \times 10^5$ cells/mL) were exposed to each compound at different concentrations for 24 h at 37 °C. The control cells were treated with vehicle (DMSO/MeOH 1:1) only. After treatment, K562 cells were washed twice with phosphate buffered saline (PBS), centrifuged (5 min, 500*g*), resuspended in 1 mL of PBS, fixed with 5 mL ice-cold 70% ethanol, and stored at 4 °C. DNA content was then measured after staining with propidium iodide (Sigma) solution (1 mL, 0.02 mg/mL propidium iodide, and 0.2 mg/mL RNase) for 30 min. Finally, the cells were analyzed using a FACSCalibur flow cytometer (Becton Dickinson), equipped with an argon-ion laser operating at a wavelength of 488 nm. The distribution of cells in the cell cycle was analyzed with the CellQuest Pro Software Version 5.2.

## ■ ASSOCIATED CONTENT

**Supporting Information.** Supporting analytical and experimental data for compounds **9a**−**9d**, **10a**, **10b**, **14a**−**14d**, **15a**, **16a**, **17a**, **18b**−**18i**, **19b**−**19i**, **21**, **23**, **27**, **28b**−**28o**, **32a**, and **34a**; methodology of the panel screen; visualization of z-scores for **28e**, **33b**, and **33c**; cell cycle analysis data of K562 cells treated with **33b** and colchicine; FACS histograms for **33c**; and table of elemental analysis results of all target compounds. This material is available free of charge via the Internet at http://pubs.acs.org.

## ■ AUTHOR INFORMATION

### Corresponding Author

*Tel: +49 251-8332195. Fax: +49 251-8332144. E-mail: prinzh@uni-muenster.de.

## ■ ACKNOWLEDGMENT

We wish to thank Roland Lindstedt, Katrin Zimmermann, Angelika Zinner and Marina Wollmann for excellent technical assistance.

## ■ ABBREVIATIONS

Akt, a serine-threonine kinase; APCI, atmospheric pressure chemical ionization; ITP, inhibition of tubulin polymerization; MTP, microtubule protein; ND, not determined; SRB, sulforhodamine B

## ■ REFERENCES

(1) Honore, S.; Pasquier, E.; Braguer, D. Understanding microtubule dynamics for improved cancer therapy. *Cell. Mol. Life Sci.* **2005**, *62*, 3039–3056.

(2) Pellegrini, F.; Budman, D. R. Review: tubulin function, action of antitubulin drugs, and new drug development. *Cancer Invest.* **2005**, *23*, 264–273.

(3) Hearn, B. R.; Shaw, S. J.; Myles, D. C. Microtubule targeting agents. *Compr. Med. Chem. II* **2007**, *7*, 81–110.

(4) Jordan, M. A. Mechanism of action of antitumor drugs that interact with microtubules and tubulin. *Curr. Med. Chem. Anticancer Agents* **2002**, *2*, 1–17.

(5) Li, Q.; Sham, H. L. Discovery and development of antimitotic agents that inhibit tubulin polymerisation for the treatment of cancer. *Expert Opin. Ther. Patents* **2002**, *12*, 1663–1702.

(6) Mahindroo, N.; Liou, J. P.; Chang, J. Y.; Hsieh, H. P. Antitubulin agents for the treatment of cancer: a medicinal chemistry update. *Expert Opin. Ther. Patents* **2006**, *16*, 647–691.

(7) Bhattacharyya, B.; Panda, D.; Gupta, S.; Banerjee, M. Antimitotic activity of colchicine and the structural basis for its interaction with tubulin. *Med. Res. Rev.* **2008**, *28*, 155–183.

(8) Duflos, A.; Kruczynski, A.; Barret, J. M. Novel aspects of natural and modified Vinca alkaloids. *Curr. Med. Chem. Anticancer Agents* **2002**, *2*, 55–70.

(9) Ferlini, C.; Gallo, D.; Scambia, G. New taxanes in development. *Expert. Opin. Invest. Drugs* **2008**, *17*, 335–347.

(10) Markman, M. Antineoplastic agents in the management of ovarian cancer: current status and emerging therapeutic strategies. *Trends Pharmacol. Sci.* **2008**, *29*, 515–519.

(11) Gridelli, C.; Aapro, M.; Ardizzoni, A.; Balducci, L.; De Marinis, F.; Kelly, K.; Le Chevalier, T.; Manegold, C.; Perrone, F.; Rosell, R.; Shepherd, F.; De Petris, L.; Di Maio, M.; Langer, C. Treatment of advanced non-small-cell lung cancer in the elderly: Results of an international expert panel. *J. Clin. Oncol.* **2005**, *23*, 3125–3137.

(12) Dhillon, T.; Stebbing, J.; Bower, M. Paclitaxel for AIDS-associated Kaposi's sarcoma. *Expert Rev. Anticancer Ther.* **2005**, *5*, 215–219.

(13) Pettit, G. R.; Singh, S. B.; Hamel, E.; Lin, C. M.; Alberts, D. S.; Garcia-Kendall, D. Isolation and structure of the strong cell growth and tubulin inhibitor combretastatin A-4. *Experientia* **1989**, *45*, 209–211.

(14) Goodin, S.; Kane, M. P.; Rubin, E. H. Epothilones: mechanism of action and biologic activity. *J. Clin. Oncol.* **2004**, *22*, 2015–2025.

(15) Yoshimatsu, K.; Yamaguchi, A.; Yoshino, H.; Koyanagi, N.; Kitoh, K. Mechanism of action of E7010, an orally active sulfonamide antitumor agent: inhibition of mitosis by binding to the colchicine site of tubulin. *Cancer. Res.* **1997**, *57*, 3208–3213.

(16) Sirisoma, N.; Kasibhatla, S.; Pervin, A.; Zhang, H.; Jiang, S.; Willardsen, J. A.; Anderson, M. B.; Baichwal, V.; Mather, G. G.; Jessing, K.; Hussain, R.; Hoang, K.; Pleiman, C. M.; Tseng, B.; Drewe, J.; Cai, S. X. Discovery of 2-chloro-N-(4-methoxyphenyl)-N-methylquinazolin-4-amine (EP128265, MPI-0441138) as a potent inducer of apoptosis with high in vivo activity. *J. Med. Chem.* **2008**, *51*, 4771–4779.

(17) Prinz, H.; Ishii, Y.; Hirano, T.; Stoiber, T.; Camacho Gomez, J. A.; Schmidt, P.; Düssmann, H.; Burger, A. M.; Prehn, J. H.; Günther, E. G.; Unger, E.; Umezawa, K. Novel benzylidene-9(10*H*)-anthracenones as highly active antimicrotubule agents. Synthesis,

antiproliferative activity, and inhibition of tubulin polymerization. *J. Med. Chem.* **2003**, *46*, 3382–3394.

(18) D'Amato, R. J.; Lin, C. M.; Flynn, E.; Folkman, J.; Hamel, E. 2-Methoxyestradiol, an endogenous mammalian metabolite, inhibits tubulin polymerization by interacting at the colchicine site. *Proc. Natl. Acad. Sci. U.S.A.* **1994**, *91*, 3964–3968.

(19) Zhang, L. H.; Wu, L.; Raymon, H. K.; Chen, R. S.; Corral, L.; Shirley, M. A.; Narla, R. K.; Gamez, J.; Muller, G. W.; Stirling, D. I.; Bartlett, J. B.; Schafer, P. H.; Payvandi, F. The synthetic compound CC-5079 is a potent inhibitor of tubulin polymerization and tumor necrosis factor-alpha production with antitumor activity. *Cancer. Res.* **2006**, *66*, 951–959.

(20) Hadfield, J. A.; Ducki, S.; Hirst, N.; McGown, A. T. Tubulin and microtubules as targets for anticancer drugs. *Prog. Cell Cycle Res.* **2003**, *5*, 309–325.

(21) Nickel, H. C.; Schmidt, P.; Böhm, K. J.; Baasner, S.; Müller, K.; Gerlach, M.; Unger, E.; Günther, E. G.; Prinz, H. Synthesis, antiproliferative activity and inhibition of tubulin polymerization by 1,5- and 1,8-disubstituted 10*H*-anthracen-9-ones bearing a 10-benzylidene or 10-(2-oxo-2-phenylethylidene) moiety. *Eur. J. Med. Chem.* **2010**, *45*, 3420–3438.

(22) Prinz, H.; Schmidt, P.; Böhm, K. J.; Baasner, S.; Müller, K.; Unger, E.; Gerlach, M.; Günther, E. G. 10-(2-*oxo*-2-Phenylethylidene)-10*H*-anthracen-9-ones as highly active antimicrotubule agents: synthesis, antiproliferative activity, and inhibition of tubulin polymerization. *J. Med. Chem.* **2009**, *52*, 1284–1294.

(23) Surkau, G.; Böhm, K. J.; Müller, K.; Prinz, H. Synthesis, antiproliferative activity and inhibition of tubulin polymerization by anthracenone-based oxime derivatives. *Eur. J. Med. Chem.* **2010**, *45*, 3354–3364.

(24) Zuse, A.; Schmidt, P.; Baasner, S.; Böhm, K. J.; Müller, K.; Gerlach, M.; Günther, E. G.; Unger, E.; Prinz, H. 9-Benzylidenenaphtho[2,3-*b*]thiophen-4-ones as novel antimicrotubule agents-synthesis, antiproliferative activity, and inhibition of tubulin polymerization. *J. Med. Chem.* **2006**, *49*, 7816–7825.

(25) Zuse, A.; Schmidt, P.; Baasner, S.; Böhm, K. J.; Müller, K.; Gerlach, M.; Günther, E. G.; Unger, E.; Prinz, H. Sulfonate derivatives of naphtho[2,3-b]thiophen-4(9*H*)-one and 9(10*H*)-anthracenone as highly active antimicrotubule agents. Synthesis, antiproliferative activity, and inhibition of tubulin polymerization. *J. Med. Chem.* **2007**, *50*, 6059–6066.

(26) Baldessarini, R. J. In *Goodman & Gilmań's The Pharmacological Basis of Therapeutics*, 11th ed.; Brunton, L. L., Lazo, J. S., Parker, K. L., Eds.; McGraw-Hill: New York, 2006; pp 429−459.

(27) Motohashi, N.; Gollapudi, S. R.; Emrani, J.; Bhattiprolu, K. R. Antitumor properties of phenothiazines. *Cancer Invest.* **1991**, *9*, 305–319.

(28) Ohlow, M. J.; Moosmann, B. Phenothiazine: the seven lives of pharmacologý's first lead structure. *Drug Discovery Today* **2011**, *16*, 119–131.

(29) Harvey, J. W.; Keitt, A. S. Studies of the efficacy and potential hazards of methylene blue therapy in aniline-induced methaemoglobinaemia. *Br. J. Hamaetol.* **1983**, *54*, 29–41.

(30) Salah, M.; Samy, N.; Fadel, M. Methylene blue mediated photodynamic therapy for resistant plaque psoriasis. *J. Drugs Dermatol.* **2009**, *8*, 42–49.

(31) Zhelev, Z.; Ohba, H.; Bakalova, R.; Hadjimitova, V.; Ishikawa, M.; Shinohara, Y.; Baba, Y. Phenothiazines suppress proliferation and induce apoptosis in cultured leukemic cells without any influence on the viability of normal lymphocytes: phenothiazines and leukemia. *Cancer Chemother. Pharmacol.* **2004**, *53*, 267–275.

(32) Okumura, H.; Nakazawa, J.; Tsuganezawa, K.; Usui, T.; Osada, H.; Matsumoto, T.; Tanaka, A.; Yokoyama, S. Phenothiazine and carbazole-related compounds inhibit mitotic kinesin Eg5 and trigger apoptosis in transformed culture cells. *Toxicol. Lett.* **2006**, *166*, 44–52.

(33) Darvesh, S.; McDonald, R. S.; Darvesh, K. V. B.; Mataija, D.; Conrad, S.; Gomez, G.; Walsh, R.; Martin, E. Selective reversible inhibition of human butyrylcholinesterase by aryl amide derivatives of phenothiazine. *Bioorg. Med. Chem.* **2007**, *15*, 6367–6378.

(34) Sobell, H. M.; Actinomycin, D. N. A. Transcription. *Proc. Natl. Acad. Sci. U.S.A.* **1985**, *82*, 5328–5331.

(35) Miyano-Kurosaki, N.; Ikegami, K.; Kurosaki, K.; Endo, T.; Aoyagi, H.; Hanami, M.; Yasumoto, J.; Tomoda, A. Anticancer effects of phenoxazine derivatives revealed by inhibition of cell growth and viability, disregulation of cell cycle, and apoptosis induction in HTLV-1-positive leukemia cells. *J. Pharmacol. Sci.* **2009**, *110*, 87–97.

(36) Motohashi, N.; Mitscher, L. A.; Meyer, R. Potential antitumor phenoxazines. *Med. Res. Rev.* **1991**, *11*, 239–294.

(37) Shimamoto, T.; Tomoda, A.; Ishida, R.; Ohyashiki, K. Antitumor effects of a novel phenoxazine derivative on human leukemia cell lines in vitro and in vivo. *Clin. Cancer Res.* **2001**, *7*, 704–708.

(38) Eregowda, G. B.; Kalpana, H. N.; Hegde, R.; Thimmaiah, K. N. Synthesis and analysis of structural features of phenoxazine analogues needed to reverse vinblastine resistance in multidrug resistant (MDR) cancer cells. *Indian J. Chem.* **2000**, *39B*, 243–259.

(39) Horton, J. K.; Thimmaiah, K. N.; Harwood, F. C.; Kuttesch, J. F.; Houghton, P. J. Pharmacological characterization of *N*-substituted phenoxazines directed toward reversing Vinca alkaloid resistance in multidrug-resistant cancer cells. *Mol. Pharmacol.* **1993**, *44*, 552–559.

(40) Thimmaiah, K. N.; Easton, J. B.; Germain, G. S.; Morton, C. L.; Kamath, S.; Buolamwini, J. K.; Houghton, P. J. Identification of N10-substituted phenoxazines as potent and specific inhibitors of Akt signaling. *J. Biol. Chem.* **2005**, *280*, 31924–31935.

(41) Kadaba, P. K.; Massie, S. P. Ring derivatives of phenothiazine. IV. Further studies on the thionation reaction, and the synthesis of phenothiazinols. *J. Org. Chem.* **1959**, *24*, 986–987.

(42) Williams, D. A. Part I: Principles of Drug Discovery. Chapter 10: Drug Metabolism. In *Foyés Principles of Medicinal Chemistry*, 6th ed.; Lemke, T. L., Williams, D. A., Eds.; Lippincott Williams & Wilkins: Philadelphia, PA, 2008; pp 253−326.

(43) Du, W.; Hardouin, C.; Cheng, H.; Hwang, I.; Boger, D. L. Heterocyclic sulfoxide and sulfone inhibitors of fatty acid amide hydrolase. *Bioorg. Med. Chem. Lett.* **2005**, *15*, 103–106.

(44) Smith, N. L. Formation and oxidation of some phenothiazine derivatives. *J. Org. Chem.* **1951**, *16*, 415–418.

(45) Eastmond, G. C.; Gilchrist, T. L.; Paprotny, J.; Steiner, A. Cyano-activated fluoro displacement reactions in the synthesis of cyanophenoxazines and related compounds. *New J. Chem.* **2001**, *25*, 385–390.

(46) Lozzio, C. B.; Lozzio, B. B. Human chronic myelogenous leukemia cell-line with positive philadelphia chromosome. *Blood* **1975**, *45*, 321–334.

(47) Fleming, F. F.; Yao, L. H.; Ravikumar, P. C.; Funk, L.; Shook, B. C. Nitrile-containing pharmaceuticals: efficacious roles of the nitrile pharmacophore. *J. Med. Chem.* **2010**, *53*, 7902–7917.

(48) Nociari, M. M.; Shalev, A.; Benias, P.; Russo, C. A novel one-step, highly sensitive fluorometric assay to evaluate cell-mediated cytotoxicity. *J. Immunol. Methods* **1998**, *213*, 157–167.

(49) Sharma, S. V.; Haber, D. A.; Settleman, J. Cell line-based platforms to evaluate the therapeutic efficacy of candidate anticancer agents. *Nat. Rev. Cancer* **2010**, *10*, 241–253.

(50) Paull, K. D.; Shoemaker, R. H.; Hodes, L.; Monks, a.; Scudiero, D. a.; Rubinstein, L.; Plowman, J.; Boyd, M. R. Display and analysis of patterns of differential activity of drugs against human-tumor cell-lines: development of mean graph and compare algorithm. *J. Natl. Cancer Inst.* **1989**, *81*, 1088–1092.

(51) Bøyum, A. Isolation of mononuclear cells and granulocytes from human blood: isolation of mononuclear cells by one centrifugation and of granulocytes by combining centrifugation and sedimentation at 1 G. *Scand. J. Clin. Lab. Invest.* **1968**, *S 21*, 77–89.

(52) Kanthou, C.; Greco, O.; Stratford, A.; Cook, I.; Knight, R.; Benzakour, O.; Tozer, G. The tubulin-binding agent combretastatin A-4-phosphate arrests endothelial cells in mitosis and induces mitotic cell death. *Am. J. Pathol.* **2004**, *165*, 1401–1411.

(53) Simoni, D.; Grisolia, G.; Giannini, G.; Roberti, M.; Rondanin, R.; Piccagli, L.; Baruchello, R.; Rossi, M.; Romagnoli, R.; Invidiata, F. P.; Grimaudo, S.; Jung, M. K.; Hamel, E.; Gebbia, N.; Crosta, L.; Abbadessa, V.; Di Cristina, A.; Dusonchet, L.; Meli, M.; Tolomeo, M. Heterocyclic

and phenyl double-bond-locked combretastatin analogues possessing potent apoptosis-inducing activity in HL60 and in MDR cell lines. *J. Med. Chem.* **2005**, *48*, 723–36.

(54) Mackie, A.; Cutler, A. A. Preparation of phenothiazine derivatives as possible anthelmintics. *J. Chem. Soc.* **1954**, 2577–2579.

(55) Turbanti, L.; DiPaco, G. F. Acyl derivatives of phenothiazine with presumed sedative action. *Boll. Chim. Farm.* **1961**, *100*, 490–495.

(56) Olmsted, M. P.; Zirkle, C. L.; Craig, P. N.; Pavloff, a. M.; Lafferty, J. J. Analogs of phenothiazines. II. Phenoxazine and phenoselenazine analogs of phenothiazine drugs. *J. Org. Chem.* **1961**, *26*, 1901–1907.

(57) Wang, M.; Gao, M.; Mock, B. H.; Miller, K. D.; Sledge, G. W.; Hutchins, G. D.; Zheng, Q.-H. Synthesis of carbon-11 labeled fluorinated 2-arylbenzothiazoles as novel potential PET cancer imaging agents. *Bioorg. Med. Chem.* **2006**, *14*, 8599–8607.

(58) Shelanski, M. L.; Gaskin, F.; Cantor, C. R. Microtubule assembly in the absence of added nucleotides. *Proc. Natl. Acad. Sci. U.S.A.* **1973**, *70*, 765–768.

(59) Vater, W.; Böhm, K. J.; Unger, E. A simple method to obtain brain microtubule protein poor in microtubule-associated proteins. *Acta Histochem. Suppl.* **1986**, *33*, 123–129.

(60) Gaskin, F.; Cantor, C. R.; Shelanski, M. L. Turbidimetric studies of the in vitro assembly and disassembly of porcine neurotubules. *J. Mol. Biol.* **1974**, *89*, 737–755.